The FASEB Journal express article 10.1096/fj.02-0453fje. Published online April 8, 2003.

Molecular analysis of Nogo expression in the hippocampus during development and following lesion and seizure

Susan Meier[1], Anja U. Bräuer[1], Bernd Heimrich[1], Martin E. Schwab[2], Robert Nitsch[1,*], and Nicolai E. Savaskan[1,*]

[1]Institute of Anatomy, Department of Cell and Neurobiology, Humboldt University Medical School Charité, Berlin, Germany; and [2]Brain Research Institute, Department of Neuromorphology, University of Zürich, and Department of Biology, Swiss Federal Institute of Technology, Zürich, Switzerland

[*]Joint senior authors.

Corresponding author: Nicolai E. Savaskan, Institute of Anatomy, Department of Cell and Neurobiology, Oskar-Hertwig House, Humboldt University Medical School Charité, Philippstr. 12, 10098 Berlin, Germany. E-mail: nicolai.savaskan@charite.de

ABSTRACT

The Nogo gene encodes an integral membrane protein mainly responsible for the neurite inhibition properties of myelin. Here, we analyzed the expression pattern of Nogo-A, Nogo-B, and Nogo-C and Nogo-66 receptor (Ng66R) mRNA during hippocampal development and lesion-induced axonal sprouting. Nogo-A and Nogo-B and Ng66R transcripts preceded the progress of myelination and were highly expressed at postnatal day zero (P0) in all principal hippocampal cell layers, with the exception of dentate granule cells. Only a slight Nogo-C expression was found at P0 in the principal cell layers of the hippocampus. During adulthood, all Nogo splice variants and their receptor were expressed in the neuronal cell layers of the hippocampus, in contrast to the myelin basic protein mRNA expression pattern, which revealed a neuronal source of Nogo gene expression in addition to oligodendrocytes. After hippocampal denervation, the Nogo genes showed an isoform-specific temporal regulation. All Nogo genes were strongly regulated in the hippocampal cell layers, whereas the Ng66R transcripts showed a significant increase in the contralateral cortex. These data could be confirmed on protein levels. Furthermore, Nogo-A expression was up-regulated after kainate-induced seizures. Our data show that neurons express Nogo genes with a clearly distinguishable pattern during development. This expression is further dynamically and isoform-specifically altered after lesioning during the early phase of structural rearrengements. Thus, our results indicate a role for Nogo-A, -B, and -C during development and during the stabilization phase of hippocampal reorganization. Taken together with these data, the finding that neurons in a highly plastic brain region express Nogo genes supports the hypothesis that Nogo may function beyond its known neuronal growth inhibition activity in shaping neuronal circuits.

Key words: axonal growth inhibitors • entorhinal cortex lesion • reticulons • kainic acid-induced seizure • axonal plasticity

Compared with the peripheral nervous system (PNS), the adult central nervous system (CNS) suffers from a lack of recovery after injury (1, 2). In general, intrinsic properties of neurons and extrinsic factors in the CNS account for the limitation in neurite growth (3). With regard to extrinsic factors, the barrier functions of lesion scarring, the presence of myelin-associated growth inhibitors, and the absence of specific guidance cues in the target area have been attributed to reduced regeneration capacity (4, 5). In contrast to the Schwann cells of the PNS, myelinating oligodendrocytes play an important role in inhibiting axonal growth. Several myelin-associated proteins show neurite growth inhibitory properties in vitro and in vivo. Among them are myelin-associated glycoprotein (MAG) (6, 7), chondroitin sulfate proteoglycans (CSPG) (8, 9), and the newly identified Nogo family, which may account for a lack of regeneration and contribute to the nonpermissive nature of the CNS after trauma (10–12). Caroni and Schwab (13, 14) showed that myelin can be converted to a more permissive axon substrate by adding the monoclonal antibody IN-1, which provided persuasive evidence for neurite growth inhibitors in myelin. IN-1 was raised against a purified 250-kDa protein named NI-250, a neurite growth inhibition activity of CNS myelin, and it also recognized a smaller inhibitory protein, NI-35. Most interestingly, IN-1 treatment of rats with spinal cord injury leads to an improvement in the regrowth of corticospinal axons and enhanced recovery of behavioral function (14–17). The antigen of IN-1, NI-250, has been purified, cloned, and renamed Nogo-A (10). The Nogo gene encodes at least three isoforms, Nogo-A, Nogo-B, and Nogo-C, resulting from both alternative promotor usage and alternative splicing (10, 18, 19). In addition, Fournier et al. (20) recently identified a receptor (Ng66R) with high affinity to the 66 amino acid residue region that is found in all three Nogo isoforms. However, the physiological function of the Nogo isoforms are still not clear, and it has been speculated that Nogo prevents excessive neuronal plasticity in the adult CNS (21, 22).

In this study, we investigated the expression of all three Nogo isoforms and their receptor in the hippocampus, a highly plastic brain region during development and after reorganization. The hippocampus is also known for its highly layer-specific innervation by entorhinal, commissural, and septal fibers (23). This layer specificity first occurs in development and is maintained even after temporal reversal of entorhinal and commissural ingrowth and during reorganization processes after lesioning (24–26). Although these studies indicate the presence of specific molecular factors both in the developing hippocampal afferent system and after deafferentation of the adult hippocampus, the molecular mechanisms and the participating molecules underlying layer-specific axonal pathfinding, growth, and restriction are not well understood (27, 28).

We extended our expression study by analyzing the Nogo transcript regulation in the hippocampus after denervation and kainate-induced axonal sprouting. In relation to this, we investigated the expression of myelin basic protein (MBP) mRNA, a reporter gene exclusively expressed by myelin-forming oligodendrocytes, and its regulation after lesioning. Hippocampal neurons expressed all three Nogo isoforms with clearly distinguishable patterns during development and adulthood. This expression was further dynamically altered after deafferentation during the early phase of structural reorganization, which indicates a role for Nogo beyond its neurite growth inhibitory activity.

MATERIAL AND METHODS

Animals and surgery

In the present study, adult male Wistar rats (200–300 g body weight), housed under standard laboratory conditions, received unilateral electrolytic lesions to the entorhinal cortex (ECL) (29). All surgical procedures were performed in agreement with German and European law on the use of laboratory animals (governmental contract Ni-344). For stereotactic surgery, rats were deeply anesthetized with a mixture of Ketanest (Gödecke/Parke-Davis, Karlsruhe, Germany), Rompun (Bayer, Leverkusen, Germany), and Ventranquil (Sanofi-Ceva, Düsseldorf, Germany) in 0.9% sterile NaCl and were placed in a stereotactic head holder (Stoelting, Hanau, Germany). A standard electrocoagulator was used to make unilateral incisions (with four single pulses (2.5 µA, 3 s each) in the frontal sagittal plane between the entorhinal cortex and hippocampus. We used the following coordinates measured from lambda: frontal incision: AP +1.2; L +3.1 to +6.1; down to the interior of the cranium; sagittal incision: AP +1.2 to +4.2; L 6.1; down to the interior of the cranium (30). Rats were allowed to survive for 1, 3, 5, 10, 15, 21, or 28 days (±0.5 day; six lesioned animals per lesion stage). We used four adult nonlesioned animals as controls.

The rats were killed by decapitation for in situ hybridization experiments. The entire brains were rapidly removed, washed in 0.1 M phosphate buffer (PB), frozen in the gaseous phase of liquid nitrogen, and stored at –80°C.

For histological staining, the animals were deeply anesthetized with an overdose of the anesthetic mixture described above and transcardially perfused with 200 ml of saline followed by 250 ml of fixative (4% paraformaldehyde [PFA] and 2% glutaraldehyde in 0.1 M PB; pH 7.5). Brains were removed and immersed in 20% sucrose dissolved in 4% PFA for 2–3 days, shock frozen with liquid nitrogen, and stored at –80°C. We cut 50 µm sections on a cryostat and stored them in 0.1 M PB.

Rats at postnatal days 17, 25, and 36 had been perfused as described above. Five-day-old rats were decapitated; their brains were removed and fixed for 2 days in 4% PFA and 2% glutaraldehyde. Afterward, the brains were immersed in 20% sucrose dissolved in 4% PFA for 2–3 days.

Kainate administration and assessments of seizure activity

Five adult male Wistar rats (Charles River, Sulzfeld, Germany), weighing 200–250 g, were used per survival stage. These animals received a single i.p. injection of kainic acid freshly dissolved in 0.9% saline (10 mg/kg of body weight; from Ocean Produce International, Shelburne, Canada). Behavior was then observed constantly for 12 h via video time-lapse recordings. Controls (two rats per survival stage) received a single i.p. injection of saline in the same volume or were not treated. Severity of seizures was scored for 4 h after kainate injection using the following classification: staring, freezing, and mouth/facial twichings were scored as 1; wet dog shakes as 2; forelimb clonus and head nodding as 3; rearing as 4; rearing and falling as 5; and jumping, circling, rolling, and wild running as 6. Only rats with seizure stages 4 or higher were studied further. Seizures at stage 6 were determined with i.p. injection with diazepam (10 mg/kg of body weight; Ratiopharm, Ulm, Germany).

Histological staining

The 50-µm-thick cryocut sections were stained with 60°C warm 0.2% solution of Black Gold (Histo-Chem, Jefferson, AR) for 35 min. To intensify the staining, sections were incubated in a solution of 0.2% potassium tertachloroaureate (Aldrich Chemical, Taufkirchen, Germany) dissolved in 0.9% NaCl for 15 min at 60°C. For fixation, the sections were then incubated for 3 min in 2% sodium thiosulfate (Merck, Berlin, Germany) solution. Between each step, the sections were carefully rinsed in 0.1 M PB (three times for 5 min each), dehydrated, and flat-embedded with Entellan (Merck). Sections were analyzed with a Zeiss Axioplan microscope (Zeiss, Jena, Germany).

In situ hybridization

For hybridization, we used an antisense oligonucleotide (5'-TTC CAC ATT AGC TCT AGC AGC CAG CAC ATC CCT ACT TC-3') complementary to the bases 1402–1440 (Nogo-A I) of the rat Nogo-A cDNA (GenBank accession number AJ242961); Nogo-A II (5'-GCT CTG GAG CTG TCC TTC ACA GGT TCT GGG GTA CTG GGG AAA GAA GC-3') 1521–1568 (31); Nogo-B (5'-TCT CTC CAG TAG AGG AGG TCA ACA ACC ACT GAG CCG GAG CCC CTG CGC TT-3') 680–730 (GenBank accession number AJ242962); Nogo-C (5'-ACT GCA AAA TTC TCC CTG AGA CAT GAA ACA CCC GCT TCC C-3') 13–53 (GenBank accession number AJ242963); Nogo-66 receptor [Ng66R] (5'-TTG TTG GCA AAC AGG TAG AGG GTC ATG AGT-3') 680–710 (GenBank accession number AY028438); Nogo-A/B (5'-TCC AGT TCC TCT AGG TCC TCG TCG TCC TCC TCC T-3') 382–416; Nogo pan (5'-GGG GAA GAC AAG TGT GAC TAC AAT GAG ATC CAT ACA CAG CAG C-3') 3922–3965 (summarized in Fig. 1); and MBP (5'-ACT ACT GGG TTT TCA TCT TGG GTC CTC TGC GAC TTC T-3') 257–294 (GenBank accession number NM017026). The Nogo-A I, Nogo-A II, Nogo-A/B, and Nogo-A pan oligonucleotides revealed essentially the same expression pattern as the Nogo-A-specific oligonucleotides alone. All oligonucleotides were synthesized by Carl Roth (Karlsruhe, Germany).

The specificity of all oligonucleotides was confirmed by a BLAST GenBank alignment search (www.nicmb.gov). Horizontal cryostat sections (20 µm) were fixed in 4% PFA, washed in 0.1 M PB (pH 7.4), and dehydrated. The oligonucleotides were end-labeled by using terminal desoxynucleotide transferase (Boehringer Mannheim, Mannheim, Germany) and [α-^{35}S]dATP (DuPont, Boston, MA). Probe labeling was performed for 10 min at 37°C. The reaction was stopped by adding 35 µl of TENS buffer (20 mM Tris [pH 8.0], 140 mM NaCl, 5 mM EDTA [pH 8.0], and 0.1% sodium dodecyl sulfate [SDS]). The radioactive probes were purified by using BioSpin6 Chromatography Columns (Bio-Rad, Munich, Germany). We used 100,000- to 300,000-cpm labeled oligonucleotides in 50 µl of hybridization buffer (50% formamide, 10 mM Tris-HCl [pH 8.0], 10 mM PB [pH 7.0], 2× standard sodium citrate (SSC), 5 mM EDTA [pH 8.0], 10% dextran sulfate, 10 mM 1,4-dithio-DL-threitol, 10 mM β-mercaptoethanol, and 200 ng/µl tRNA) per section.

Hybridization was performed for 16 h at 42°C in a humidified chamber, after which the slides were washed as follows: 1× 60 min in 0.1× SSC at 56°C and 1× 5 min in 0.05× SSC at room temperature. Finally, sections were rinsed in H_2O at room temperature and dehydrated in 50%, 75%, and 96% ethanol. For autoradiography, slides were exposed to Kodak X-OMAT AR X-ray

films (Amersham Pharmacia Biotech, Heidelberg, Germany) for 5–21 days. No signals were detected on sections hybridized with specific antisense oligonucleotide when unlabeled oligonucleotide was added in 100-fold surplus or with sense probes of the respective oligonucleotides.

After exposure of sections, they were stained with Nissl stain as described previously (32). In brief, following in situ hybridization, sections were rehydrated in a decreasing concentration ethanol series, washed in PBS, counterstained with Nissl stain (cresyl violet acetate, Sigma, Rödermark, Germany), dehydrated through an ascending series of ethanol, flat-embedded with Hypermount, and covered with coverslips. Sections were then digitally photographed (Zeiss Axioplan).

Quantification of autoradiography

Six animals were analyzed by in situ hybridization for each of the seven postlesion and four of the unlesioned control values as described earlier (29). For each animal and each transcript analyzed, at least two in situ hybridization autoradiographs of adjacent brain slices were used for the quantification of signal strength. The autoradiographs were digitalized via a scanner (Micotek ScanMaker 636; Microtek, Carson, CA). To quantify the intensity on an pixel level, we used the computerized videodensometry system (Metamorph, Universal Imaging, Downingtown, PA). A visually established pixel intensity threshold was set to remove the unlabeled portion of the image. The standard rectangle (1.5 mm^2) was defined and placed in 15 different positions over the pyramidal cell layers of the cornu ammonis (CA) CA1 and CA2/CA3, the granule cell layer of the dentate gyrus, the hilus, and the cortex. A mean value of the 15 measurements was calculated for each region and set in reference to the unlesioned controls (100%). Analysis was performed with the Mann-Whitney *U* test (StatView II, Abacus Concepts, Berkeley, CA). The level of significance was set at $*P < 0.05$, $**P < 0.01$, and $***P < 0.001$.

Nonradioactive in situ hybridization

For in situ hybridization experiments, brains were dissected and frozen in the gaseous phase of liquid nitrogen. Horizontal cryostat sections (20 μm) were fixed in 65°C warm 1× PBS for 10 min and in 4% PFA dissolved in 1× PBS for 15 min, and they were washed twice in active 0.1% diethylpyrocarbonate (DEPC) in 1× PBS and in 5× SSC for another 15 min. Prehybridization was performed for 2 h at 25°C with 200 μl of hybridization buffer (25% formamide, 4× SSC, 5× Denhardts, 50 mM NaH_2PO_4/Na_2HPO_4, pH 7, 0.1 mM EDTA), 1 mg/ml herring sperm, and 1 mg/ml yeast tRNA. Afterward, slices were washed twice for 10 min each time with 2× SSC and hybridized for 16 h at 25°C in 200 μl of hybridization buffer, 1 mg/ml herring sperm, 1 mg/ml yeast tRNA, and 1 μg of the antisense digoxigenin (Dig)-labeled oligonucleotide (5'-Dig-ACA TTA GCT CTA GCA GCC AGC ACA TCC CTA-3') complementary to the bases 1406–1436 of the rat Nogo-A cDNA (synthezised by Tip Molbiol, Munich, Germany; the specificity was confirmend by BLAST GenBank [www.ncbi.nlm.nih.gov/BLAST/]). A noncomplementary (sense) probe served as a control. The sections were washed 2× 15 min in 2× SSC, 2× 20 min in 1× SSC, and 3× 30 min in 0.25× SSC. The slices were rinsed 2× 5 min in Dig1 solution (100 mM Tris and 150 mM NaCl; pH 7.5) and then blocked for 30 min in Dig2 (1% blocking solution [Roche 1093657; Roche, Basel, Switzerland] dissolved in Dig1). Alkaline phosphatase-coupled anti-digoxigenin antibody (IgG, 1:1000 solved in Dig1; Roche) was incubated for 2 h at room

temperature. The slides were washed 3× 15 min in Dig1 and 1× 15 min Dig3 (100 mM Tris-HCl, pH 9.5, 100 mM NaCl, 50 mM $MgCl_2$). The staining was developed overnight at 25°C in 4-nitroblue tetrazolium chloride/5-bromo-4-chloro-3-indolyl phosphate (NBT/BCIP) stock solution (DIG Nucleic Acid Detection Kit, Roche) and 1 mM levamisole solved in Dig3. The reaction was stopped with Dig4 (10 mM Tris-HCl and 10 mM EDTA, pH 7.5) for 1 min. The sections were then whipped for 30 s in distilled water and hydrated for 30 min in tap water. The sections were counterstained with the fluorescent Nissl dye (Molecular Probes, Eugene, OR) for 5 min, washed in PBS, subsequently stained with the nuclear dye Hoechst 33528 (Frankfurt am Main, Germany) (1:12000) for 2 min, and mounted without drying with HydroMount (National Diagnostics, Atlanta, GA).

Immunoblots

Total protein extracts from hippocampi were prepared as described earlier (10); proteins were subjected to SDS-polyacrylamide gel electrophoresis on 12% polyacrylamide gel. Twenty micrograms of the soluble fraction was loaded per lane. The separated proteins were then electroblotted onto a Hybond ECL nitrocellulose membrane (Amersham Pharmacia Biotech). Immunoanalysis was performed with a mouse anti-Nogo-A monoclonal antibody (αRatII-C7) detecting a 205-kDa band, and for equal loading controls a mouse β-actin monoclonal antibody (Sigma) was used. Myosin (212 kDa), MBP-β-galactosidase (158 kDa), and maltose binding protein 2 (42 kDa) were used as protein molecular size references. Immunoblots and ponceau-stained gels were quantified by densiometry by using Metamorph (Universal Imaging). Analysis was performed with the Mann-Whitney *U* test (Statview II, Abacus). The level of significance was set at $*P < 0.05$, $**P < 0.01$, $***P < 0.001$.

RESULTS

Appearance of myelinated fibers in the hippocampus during development

We first investigated the distribution of myelinated fibers in the developing hippocampal formation by means of Black Gold, a specific marker for myelin. There were no myelinated fibers present in the hippocampus at postnatal day 0 (P0) (Fig. 2B). At P5, only a slight, patch-like diffuse staining was visible in the entire hippocampal area (Fig. 2C). Myelinated fibers were first detectable in the stratum lacunosum-moleculare of the CA3 region at P17 (Fig. 2D). The myelination in the entorhinal termination zones was completed at P25 (Fig. 2E, F).

Conversely, expression of a prominent myelin component MBP mRNA was first found in the hippocampal neuropil at P15 (Fig. 3). At P30, the most densely populated areas of MBP mRNA expression were the strata oriens and radiata of the CA regions. Noteworthy is that the hybridization signals for MBP mRNA were hardly found in any of the hippocampal neuronal cell layers (Fig. 3; see Fig. 13).

Nogo-A, -B, and -C and Ng66R expression during hippocampal development

Nogo-A, Nogo-B, and Ng66R mRNA expression signals were first detected in the developing brain at P0, the earliest developing time point investigated in our study (Fig. 3). At this stage, an intense hybridization signal was found in the pyramidal cells from CA1 to CA3, and a brighter

signal was detectable in the presubiculum. Nogo-A, Nogo-B, and Ng66R mRNAs were expressed only very slightly in the granule cell layer of the dentate gyrus at this time point. No signals were detectable in the molecular layer and in the strata lucidum, radiata, lacunosum-moleculare, and oriens. The mRNA distribution of Nogo-A and Ng66R remained unchanged from P15 to adulthood, with the exception of Ng66R mRNA signals in the hilar region, which declined during adulthood. The Nogo-B transcripts were found in the hippocampus proper until adulthood. However, Nogo-B mRNA levels declined during maturation in the cortex and subiculum (Fig. 3).

We found barely any Nogo-C mRNA signal in any of the neuronal cell layers of the hippocampus at P0 to P5. We first found Nogo-C mRNA expression in the neuronal cell layer of the dentate gyrus and the CA1-CA3 region at P15, but we found hardly any hybridization signal in the hilar region and entorhinal cortex. This expression pattern remained unchanged until adulthood (Fig. 3).

Nogo-A mRNA expression was located in neuronal cell layers of the hippocampal formation

Because the expression patterns of the Nogo gene and its splice variants were distributed in cell layers that are known for neuron residence, we proceeded to test mRNA expression on the cellular level. Using nonradiolabeled probes for Nogo-A transcripts, we revealed its distribution in the pyramidal and granule cells of the hippocampus (Fig. 4) and in entorhinal neurons of layer II-IV beside oligodendrocytes in white matter (Fig. 4A, E). Granule cells in the dentate gyrus that were Nissl-positive gave a strong hybridization signal, whereas only a few Nogo-A-stained cells could be detected in the hippocampus neuropil (Fig. 4D).

Nogo-A, -B, and -C, Ng66R, and MBP mRNA expression after hippocampal deafferentation

We continued by analyzing the expression patterns of Nogo genes and receptor in the adult hippocampus after denervation. In adult nonlesioned control animals, Nogo-A mRNA was predominantly expressed in the pyramidal cell layers of the CA1 to CA3 region and to an lesser extent in the dentate gyrus (Fig. 5A; Fig. 6; see Fig. 12). A massive increase of Nogo-A mRNA levels first occurred 1 day after lesion (1 dal). At this time point, a more than 20-fold increase was visible in the ipsilateral and contralateral cortex. This evident upregulation peaked at 34-fold of the control levels at 5 dal on the ipsilateral side and at 3 dal on the contralateral side (Fig. 5A, B). Subsequent Nogo-A mRNA content decreased at longer survival stages and reached control levels at 28 dal. In the hippocampus, the granule cell layer ipsilateral to the lesion side showed an increase of the mRNA content as early as 1 dal and remained up-regulated until 10 dal. Expression decreased at 15 dal in comparison to control levels, whereas the contralateral side did not show any alterations. The pyramidal cells of the CA1 region did not show alterations in Nogo-A expression compared with controls. However, a significant increase in Nogo-A mRNA levels was found in the pyramidal cells of CA3 from the earliest lesion stage to 10 dal and declined at 15 dal. The hilar region of the ipsi- and contralateral hippocampus showed a more than 30-fold increase during the early phase after lesioning and subsequently decreased below control levels at 15 and 21 dal. There was no obvious alteration of Nogo-A mRNA expression at longer survival stages (Fig. 5 A, B).

In general, the Nogo-B hybridization pattern was less prominent in the hippocampus compared with the Nogo-A hybridization pattern (Fig. 7A, Fig. 8). The highest Nogo-B mRNA concentration was detected in the pyramidal cells of the CA regions, and a weak signal was seen in the dentate gyrus. The Nogo-B mRNA concentration of the ipsilateral cortex increased at 1 dal, reached nearly 20-fold of the control level at 3 dal, decreased afterward, and reached the control level at 10 dal. The contralateral cortex showed a slight but significant upregulation at 3 dal, decreased afterward, and reached the control level at 10 dal. A significant upregulation of the Nogo-B transcript appeared in all cell layers of the hippocampus in the early phase of reorganization and returned to control levels at a time point when axonal sprouting processes peaked (Fig. 7A, B; Fig. 12). The granule cell layer and the hilar region ipsilateral to the lesion showed the highest hybridization signal 1 dal and declined to control levels at 15 dal. On the same side, the pyramidal cells of the CA1-CA3 region showed an intense Nogo-B hybridization signal at 1 dal. Whereas the Nogo-B mRNA expression the CA1 region reached control levels at 5 dal, expression levels in CA3 remained significantly up-regulated and reached control levels at 28 dal. On the contralateral side, the granule cell layer of the dentate gyrus and pyramidal cell layer of the CA3 region showed a significant increase in Nogo-B transcription but other hippocampal subfields were unaltered. The contralateral upregulation of Nogo-B mRNA was evident until 10 dal (Fig. 7A, B).

Nogo-C mRNA was not regulated in cortical regions at any time point after ECL (data not shown). Nogo-C expression of the ipsilateral hippocampal cell layers started to increase during the early lesion stages when glial activity commences and showed a peak at 3 dal (Fig. 9A, B). With exception of the hilar region, the Nogo-C mRNA later decreased to below control levels at 10 dal and recovered to nonlesioned control levels at 28 dal. An upregulation of the mRNA in the ipsilateral hilar region could be measured starting 1 dal, peaked significantly at 5 dal, and reached control levels at 28 dal (Fig. 9A, B; see Fig. 12).

Ng66R mRNA was significantly up-regulated in the cortex after lesioning (Fig. 10A, B; Fig. 11). Whereas this alteration reached its maximum at 1 dal on both sides of the lesion, the ipsilateral cortex returned to control levels at 3 dal, whereas the contralateral side remained high until 28 dal. The ipsilateral granule cell layer and all contralateral hippocampal cell layers showed a biphasic time course of Ng66R mRNA, with a maximum peak at 3 dal and the maximum decrease at 15 dal. There was no visible regulation at 28 dal in comparison to the values of the adult controls. The ipsilateral hilar region showed no regulation at any time point after lesioning. The pyramidal cells of the CA3 and CA1 region showed a slight upregulation of the Ng66R mRNA at 1 dal (Fig. 10A, B; Fig. 12).

In comparison to the Nogo ligands and their receptor, MBP mRNA was not found in any principal cells of the hippocampus at any time point (Fig. 13A, B). Around the lesion area, MBP mRNA was up-regulated starting from 1 dal. In the hilar region, MBP mRNA demonstrated a significant upregulation from 1 dal on. A peak was reached at 15 dal, and the mRNA concentration decreased rapidly to control levels at 28 dal. MBP mRNA also increased constantly in the strata radiata and oriens of the CA region beginning from 1 dal. A maximal peak was reached between 10 and 15 dal, and the control level was reached at 28 dal. MBP transcripts did not show any alteration in the contralateral hippocampus at any of the time points we investigated (Fig. 13A, B).

That the altered Nogo gene expression indeed led to changed protein expression levels and therefore has biological consequences could be shown by immunoblots. We found a significant upregulation of Nogo-A in the hippocampus (Fig. 14). Also, the level of Nogo-A protein expression was developmentally regulated, with high levels at postnatal stages (Fig. 14).

Nogo-A mRNA expression was regulated after kainate-induced seizures

We tested the expression levels of Nogo-A in another model of synaptic plasticity. During the first day after kainate-induced seizures, in which neuronal apoptosis and axonal degeneration dominate, no expression alteration could be found (Fig. 15). However, at 5 days postseizure (dps), at a time point known for GAP-43 reexpression, significant upregulation of Nogo-A mRNA occurred in principal neurons of the hippocampus (Fig. 15).

DISCUSSION

Using in situ hybridization, we analyzed the mRNA expression of the three Nogo isoforms and their receptor in the developing and adult hippocampus and after transection of the perforant path. We could demonstrate that the most prominent expression signal of Nogo-A, Nogo-B, and Nogo-C could be found in the neuronal cell layers of the hippocampus. With exception of Nogo-C mRNA, both Nogo-A and Nogo-B and Ng66R were present in the hippocampus starting from the day of birth (P0). After CNS injury, they were regulated differently, which indicates an important neuronal role during development and adulthood and after lesioning, in addition to their myelin-associated neurite growth inhibition activities.

Nogo genes during hippocampal development

During CNS development, axons extend from cells within the CNS and form an intricate and specific web of connections (33). During hippocampal development, stellate and pyramidal cells from layers II and III of the entorhinal cortex send their main fibers to the outer molecular layer of the dentate gyrus and the stratum lacunosum-moleculare via the perforant pathway (34, 35). First, entorhinal axons arrive at their final target in late embryonic stages in a layer-specific manner, segregating in the outermost part of the dentate molecular layer (23–25, 36). Thereafter, the entorhinal terminals are restricted specifically to this layer throughout adulthood and respect termination zones of other afferents, i.e., commissural fiber projections (25, 37). The myelination process of entorhinal afferents in the hippocampal area commences during the second postnatal week (P15) and is completed by P60 (38, 39). However, Nogo-A, Nogo-B, and Ng66R mRNA expression occurred far before myelination took place in the neuropil of the hippocampus. The first hybridization signals for Nogo-A, Nogo-B, and Ng66R mRNA could be found in the entorhinal cortex and CA regions of the hippocampus at P0, the earliest time point investigated.

Nogo-C and MBP mRNA were first significantly expressed in the hippocampus at P15, a time point when the first myelinating fibers appear (39). However, in contrast to MBP expression, which was exclusively located in white matter regions, Nogo-C mRNA expression was predominantly found in principal cell layers of the hippocampus and to a lesser extent in the neuropil. This observation could be explained by the low metabolic activity of oligodendrocytes in contrast to that of neurons (40). Another interesting fact is that Nogo-C transcripts were first found in the dentate gyrus at a time when the later occurring infrapyramidal dentate blade has

developed and granule cells have differentiated to a mature state (41). This maturation-dependent expression in connection with the lack of neurite growth-inhibitory activity of recombinant Nogo-C and its proposed intracellular localization indicate a function different from cell surface signaling (42).

As shown by nonradioactive in situ hybridization, Nogo-A mRNA was found in all neuronal cell layers of the entorhino-hippocampal system. This observation was confirmed by double immunostaining for Nogo-A and calbindin and parvalbumin, respectively, which demonstrated Nogo-A expression by dentate granule cells and hilar interneurons (43). Interestingly, Ng66R was also expressed in the entorhinal cortex and subiculum from P0 through to adulthood. At the same time point (P0), entorhinal axons invade the hippocampus and specifically segregate in the outermost layers of the hippocampus (25). This correlation might be due to a novel receptor-ligand system, which may control the layer-specific termination of hippocampal afferents. In this regard, it is conceivable that Nogo-A acts as a repulsive or attractive cell surface signal on neurons and their extensions as well as on non-neuronal cells. However, it is also possible that Nogo-A functions bidirectionally as a receptor. Such signaling is also known for another class of guidance molecules, the ephrins and Eph receptors, which are involved in entorhinal pathfinding, leading to lamina-specific restriction in the hippocampus (44–47).

Nogo gene expression after ECL

The mature CNS is a nonpermissive environment for outgrowing axons in contrast to the PNS, which accounts for the limited regeneration capacity after lesioning (1, 48). The fiber projection of the entorhinal cortex is a major cortical pathway to the hippocampus (49). Early degeneration of the entorhinal neurons in the progress of Alzheimer disease results in a layer-specific denervation of the hippocampus, leading to a loss of memory function (50, 51). An ipsilateral transection of the perforant path results in an anterograde degeneration of entorhinal axons and synapses in the outer molecular layer of the dentate gyrus and stratum lacunosum-moleculare of the CA1 and CA3, followed by a rapid activation of microglial and astroglial cells (52, 53). This is followed by reactive sprouting of the remaining axons, leading to the reappearance of intact synapses to almost normal levels (54, 55). However, the molecular mechanisms of such layer-specific axon growth in response to a lesion are only poorly understood. It is known that some guidance molecules involved in pathfinding during development also demonstrate upregulation of mRNA after CNS damage (56–60).

All Nogo splice variants were strongly regulated after ECL. Nogo-A, Nogo-B, and Ng66R were up-regulated in the ipsilateral cortex, the region where lesion-induced cell death and transneuronal alterations occur (61, 62). However, Ng66R transcripts were also strongly up-regulated in the contralateral cortex.

In the hippocampus, the Nogo genes showed an isoform-specific regulation after a perforant path lesion. The granule cells of the dentate gyrus, which are the first relay station in the hippocampal trisynaptic pathway affected by ECL, showed a strong increase in mRNA content of all Nogo transcripts and their receptor during the time point at which wallerian degeneration commences and neuronal and glial responses start (63). During the time period when degenerative processes and glial phagocytotic activity were at their maximum (2–8 dal), Nogo-B mRNA concentration in the granule cell layer had already reached control levels, but Nogo-A remained up-regulated.

Meanwhile, Nogo-C and Ng66R mRNA levels began to decrease and showed a significant downregulation during the time of axonal sprouting and termination [6–12 dal; (64)]. Interestingly, at the time point at which axonal sprouting and synaptic formation peak, expression levels of Nogo-A and Nogo-B transcripts reached control levels. In contrast, Nogo-C and Ng66R mRNA levels remained suppressed and first reached control levels after axonal sprouting process commenced. Conversely, in the contralateral hippocampus, which is one major origin of sprouting neurites (55, 65), Ng66R mRNA was significantly reduced during the phase of axonal sprouting. This decreased Ng66R expression correlates well with the time of axon ingrowth into the lesioned hippocampus, if a transiently reduced axonal responsiveness to the neurite growth-inhibitor Nogo-A is assumed. Further, this regulation seems to be specific because Nogo-B and Nogo-C mRNA did not show any alteration in response to a lesion at this time point. It was recently shown that Ng66R is also the receptor for oligodendrocyte-myelin glycoprotein and mediates its neurite outgrowth and growth cone collapse activity (66). Thus, downregulation of Ng66R is sufficient to attenuate Nogo-mediated neurite growth inhibition because axons that do not express Ng66R are insensitive to growth cone collapse induction by Nogo (20). The fact that Nogo genes could be involved in structural plasticity is indicated in the kainate-induced seizure model. In this model of increased synaptic activity, we found increased Nogo-A expression specifically at the time point at which supragranular axon sprouting and GAP-43 expression occur in the hippocampus (67).

Functional consequences of Nogo expression changes after ECL

The monoclonal antiboby IN-1, which recognizes the myelin protein components of 250 and 35 kDa, prevents growth cone collapse and allows neurite outgrowth on a CNS myelin or oligodendrocyte substrate and neurite ingrowth into optic nerve explants (14). In vivo applications in brain or spinal cord result in a long-distance regeneration of small proportions of adult CNS axons (15, 68–70). Spinal cord-lesioned animals showed a significant functional improvement in specific locomotory and reflex tasks after monoclonal antibody IN-1 application (16).

The Nogo genes have been identified as a new member of the reticulon family and are thereby alternatively called reticulon 4 (10, 18). The 188 C-terminal amino acids of the Nogo family are about 70% identical across the reticulon family. Like the other reticulons, Nogo-A is associated with the endoplasmatic reticulum (18, 68; A. B. Huber, M. E. van der Haar, and M. E. Schwab, unpublished observations). Reticulon 1 and reticulon 3 are not expressed by oligodendrocytes, in comparison to Nogo-A, which is expressed by most but not all oligodendrocytes (18). The hydrophobic segments—the 66-residue extracellular domain of the common C terminus and an area in the N terminus of Nogo-A—contain functionally important residues. In contrast, the 66-residue luminal/extracellular domains from reticulons 1, 2, and 3 do not inhibit axonal regeneration.

The normal role of the Nogo system under physiological conditions is not yet fully elucidated. A cell surface signal with attractive and repulsive functions to other neurons, neurites, or non-neuronal cells has been assumed. So far, it has been suggested that Nogo-A, similar to netrin-1 and slit, is involved in cerebellar granule cell migration (43, 71, 72). Also, Nogo-A, -B, and -C would function in an intracellular manner in neurons, as indicated by the reticulon expression pattern. Similar to reticulon-1, the Nogo genes could be involved in protein transfer, protein

packaging and trafficking, and regulation of intracellular calcium levels (73, 74). It was recently shown that the putative extracellular domain of the common C terminus of Nogo interacts with a novel mitochondrial preprotein (NIMP) and with ubiquinolcytochrome *c* reductase core proteins 1 and 2 (75). These data support the idea that Nogo is involved in protein trafficking, at least in pathological conditions. Whether this finding is significant for all isoforms of Nogo remains to be shown. Also, Nogo MAG and oligodendrocyte-myelin glycoprotein are functional ligands for Ng66R (66, 76). Furthermore, the neurotrophin growth factor receptor p75 interacts with Ng66R as a coreceptor for the ligands Nogo, MAG, and oligodendrocyte-myelin glycoprotein, which suggests that p75 is the executive tranducer of the Ng66R-mediated activation into the cell interior (77).

The early mRNA expression of all Nogo transcripts during hippocampal development indicates a strong physiological role in addition to axonal growth inhibition (78, 79). Interestingly, all Nogo transcripts and their receptor were located predominantly in neurons from postnatal stages on. It could be suggested that because of the complementary expression of the Nogo ligands and the Ng66R during hippocampal development, they form a novel receptor-ligand system that determines axonal pathfinding, which leads to a lamina-specific restriction and termination pattern (Fig. 16). This is also known for repulsive guidance cues, such as semaphorin 3A (Sema3A) or ephrin 3A, in lamina-specific pathfinding of entorhinal axons (45, 80, 81).

Furthermore, it was shown that Nogo-A and Ng66R are located at sites of axon myelin and synapses (82). Together with our findings of an activity-dependent regulation of Nogo, this result suggests that it is plausible that the Nogo system may contribute to structural plasticity such as axonal and dendritic spine rearrangements.

Recently, the Strittmatter group showed that Ng66R inhibition by a peptide antagonist results in significant axonal outgrowth promotion and improves functional recovery after a spinal cord lesion (12). However, neutralization of Nogo activity also results in increased plasticity and excessive sprouting in noninjured CNS fibers (21, 22, 83). Thus, our data on neuronal Nogo gene expression under physiological conditions should be significant when application of Nogo neutralization antibodies or Nogo receptor inhibitors to therapeutic approaches in the CNS is considered.

ACKNOWLEDGMENTS

We thank Sabine Lewandowski and Dore Wachenschwanz for photographic and digital art work. Miriam Petzold is mentioned for technical assistance. The authors are grateful to Andrea B. Huber for sharing unpublished data. This study was supported by the German Research Council (DFG: SFB 515/A5 to R. N. and He-1520 to B. H.). N. E. S. is an Investigator of the Charité Medical Research Foundation.

REFERENCES

1. David, S., and Aguayo, A. J. (1981) Axonal elongation into peripheral nervous system "bridges" after central nervous system injury in adult rats. *Science* **214,** 913–933

2. Schwab, M. E., and Bartholdi, D. (1996) Degeneration and regeneration of axons in the lesioned spinal cord. *Physiol. Rev.* **76,** 319–370

3. Horner, P. J., and Gage, F. H. (2000) Regenerating the damaged central nervous system. *Nature (London)* **407,** 963–970

4. Fournier, A. E., GrandPre, T., Gould, G., Wang, X., and Strittmatter, S. M. (2002) Nogo and the Nogo-66 receptor. *Prog. Brain Res*. **137,** 361–369

5. Skaper, S. D., Moore, S. E., and Walsh, F. S. (2001) Cell signalling cascades regulating neuronal growth-promoting and inhibitory cues. *Prog. Neurobiol.* **65,** 593–608

6. McKerracher, L., David, S., Jackson, D. L., Kottis, V., Dunn, R. J., and Braun, P. E. (1994) Identification of myelin-associated glycoprotein as a major myelin-derived inhibitor of neurite growth. *Neuron* **13,** 805–811

7. Mukhopadhyay, G., Doherty, P., Walsh. F. S., Crocker, P. R., and Filbin, M. T. (1994) A novel role for myelin-associated glycoprotein as an inhibitor of axonal regeneration. *Neuron* **13,** 757–767

8. Dou, C. L., and Levine, J. M. (1994) Inhibition of neurite growth by the NG2 chondroitin sulfate proteoglycan. *J. Neurosci.* **14,** 7616–7628

9. Niederost, B. P., Zimmermann, D. R., Schwab, M. E., and Bandtlow, C. E. (1999) Bovine CNS myelin contains neurite growth-inhibitory activity associated with chondroitin sulfate proteoglycans. *J. Neurosci.* **19,** 8979–8989

10. Chen, M. S., Huber, A. B., van der Haar, M. E., Frank, M., Schnell, L., Spillmann, A. A., Christ, F., and Schwab, M. E. (2000) Nogo-A is a myelin-associated neurite outgrowth inhibitor and an antigen for monoclonal antibody IN-1. *Nature (London)* **403,** 434–439

11. GrandPre, T., and Strittmatter, S. M. (2001) Nogo: a molecular determinant of axonal growth and regeneration. *Neuroscientist* **7,** 377–386

12. GrandPre, T., and Strittmatter, S. M. (2002) Nogo-66 receptor antagonist peptide promotes axonal regeneration. *Nature (London)* **417,** 547–551

13. Caroni, P., and Schwab, M. E. (1988) Antibody against myelin-associated inhibitor of neurite growth neutralizes nonpermissive substrate properties of CNS white matter. *Neuron* **1,** 85–96

14. Caroni, P., and Schwab, M. E. (1988) Two membrane protein fractions from rat central myelin with inhibitory properties for neurite growth and fibroblast spreading. *J. Cell Biol.* **106,** 1281–1288

15. Schnell, L., and Schwab, M. E. (1990) Axonal regeneration in the rat spinal cord produced by an antibody against myelin-associated neurite growth inhibitors. *Nature (London)* **343,** 269–272

16. Bregman, B. S., Kunkel-Bagden, E., Schnell, L., Dai, H. N., Gao, D., and Schwab, M. E. (1995) Recovery from spinal cord injury mediated by antibodies to neurite growth inhibitors. *Nature (London)* **378,** 498–501

17. Brosamle, C., Huber, A. B., Fiedler, M., Skerra, A., and Schwab, M. E. (2000) Regeneration of lesioned corticospinal tract fibers in the adult rat induced by a recombinant, humanized IN-1 antibody fragment. *J. Neurosci.* **20,** 8061–8068

18. GrandPre, T., Nakamura, F., Vartanian, T., and Strittmatter, S. M. (2000) Identification of the Nogo inhibitor of axon regeneration as a Reticulon protein. *Nature (London)* **403,** 439–444

19. Prinjha, R., Moore, S. E., Vinson, M., Blake, S., Morrow, R., Christie, G., Michalovich, D., Simmons, D. L., and Walsh, F. S. (2000) Inhibitor of neurite outgrowth in humans. *Nature (London)* **403,** 383–384

20. Fournier, A. E., GrandPre, T., and Strittmatter, S. M. (2001) Identification of a receptor mediating Nogo-66 inhibition of axonal regeneration. *Nature (London)* **409,** 341–346

21. Buffo, A., Zagrebelsky, M., Huber, A. B., Skerra, A., Schwab, M. E., Strata, P., and Rossi, F. (2000) Application of neutralizing antibodies against NI-35/250 myelin-associated neurite growth inhibitory proteins to the adult rat cerebellum induces sprouting of uninjured Purkinje cell axons. *J. Neurosci.* **20,** 2275–2286

22. Zagrebelsky, M., Buffo, A., Skerra, A., Schwab, M. E., Strata, P., and Rossi, F. (1998) Retrograde regulation of growth-associated gene expression in adult rat Purkinje cells by myelin-associated neurite growth inhibitory proteins. *J. Neurosci.* **18,** 7912–7929

23. Skutella, T., and Nitsch, R. (2001) New molecules for hippocampal development. *Trends Neurosci.* **24,** 107–113

24. Frotscher, M., and Heimrich, B. (1993) Formation of layer-specific fiber projections to the hippocampus in vitro. *Proc. Natl. Acad. Sci. USA* **90,** 10400–10403

25. Super, H., and Soriano, E. (1994) The organization of the embryonic and early postnatal murine hippocampus. II. Development of entorhinal, commissural, and septal connections studied with the lipophilic tracer DiI. *J. Comp. Neurol.* **344,** 101–120

26. Deller, T., and Frotscher, M. (1997) Lesion-induced plasticity of central neurons: sprouting of single fibres in the rat hippocampus after unilateral entorhinal cortex lesion. *Prog. Neurobiol.* **53,** 687–727

27. Frotscher, M., Heimrich, B., and Deller, T. (1997) Sprouting in the hippocampus is layer-specific. *Trends Neurosci.* **20,** 218–223

28. Savaskan, N. E., and Nitsch, R. (2001) Molecules involved in reactive sprouting in the hippocampus. *Rev. Neurosci.* **12,** 195–215

29. Brauer, A. U., Savaskan, N. E., Kole, M. H., Plaschke, M., Monteggia, L. M., Nestler, E. J., Simburger, E., Deisz, R. A., Ninnemann, O., and Nitsch, R. (2001) Molecular and functional analysis of hyperpolarization-activated pacemaker channels in the hippocampus after entorhinal cortex lesion. *FASEB J.* **15,** 2689–2701

30. Paxinos, G., Watson, C., Pennisi, M., and Topple, A. (1985) Bregma, lambda and the interaural midpoint in stereotaxic surgery with rats of different sex, strain and weight. *J. Neurosci. Methods* **13,** 139–143

31. Josephson, A., Widenfalk, J., Widmer H. W., Olson L., and Spenger, C. (2001) NOGO mRNA expression in adult and fetal human and rat nervous tissue and in weight drop injury. *Exp Neurol.* **169,** 319–328

32. Savaskan, N. E., Alvarez-Bolado, G., Glumm, R., Nitsch, R., Skutella, T., and Heimrich, B. (2002) Impaired postnatal development of hippocampal neurons and axon projections in the $Emx2^{-/-}$ mutants. *J. Neurochem.* **83,** 1196–1207

33. Tessier-Lavigne, M., and Goodman, C. S. (1996) The molecular biology of axon guidance. *Science* **274,** 1123–1133

34. Steward, O. (1976) Reinnervation of dentate gyrus by homologous afferents following entorhinal cortical lesions in adult rats. *Science* **194,** 426–428

35. Bayer, S. A., and Altman, J. (1990) Development of layer I and the subplate in the rat neocortex. *Exp. Neurol.* **107,** 48–62

36. Skutella, T., Savaskan, N. E., Ninnemann, O., and Nitsch, R. (1999) Target- and maturation-specific membrane-associated molecules determine the ingrowth of entorhinal fibers into the hippocampus. *Dev. Biol.* **211,** 277–292

37. Snyder, D. C., Coltman, B. W., Muneoka, K., and Ide, C. F. (1991) Mapping the early development of projections from the entorhinal cortex in the embryonic mouse using prenatal surgery techniques. *J. Neurobiol.* **22,** 897–906

38. Suzuki, M., and Raisman, G. (1994) Multifocal pattern of postnatal development of the macroglial framework of the rat fimbria. *Glia* **12,** 294–308

39. Savaskan, N. E., Plaschke, M., Ninnemann, O., Spillmann, A. A., Schwab, M. E., Nitsch, R., and Skutella, T. (1999) Myelin does not influence the choice behaviour of entorhinal axons but strongly inhibits their outgrowth length in vitro. *Eur. J. Neurosci.* **11,** 316–326

40. Rust, R.-S. J., Carter, J. G., Martin, D., Nerbonne, J. M., Lampe, P. A., Pusateri, M. E., and Lowry, O. H. (1991) Enzyme levels in cultured astrocytes, oligodendrocytes and Schwann cells, and neurons from the cerebral cortex and superior cervical ganglia of the rat. *Neurochem. Res.* **16,** 991–999

41. Blackstad, T. W. (1956) Commissural connections of the hippocampal region in the rat, with specific reference to their mode of termination. *J. Comp. Neurol.* **105,** 417–537

42. Oertel, T., Bandtlow, C. E., and Schwab, M. E. (2000) Characterization of the gene structure and the inhibitory regions of Nogo/RTN4. *Soc. Neurosci. Abstr.* **26,** 573

43. Huber, A. B., Weinmann, O., Brosamle, C., Oertle, T., and Schwab, M. E. (2002) Patterns of Nogo mRNA and protein expression in the developing and adult rat and after CNS lesions. *J. Neurosci.* **22,** 3553–3567

44. Holder, N., and Klein, R. (1999) Eph receptors and ephrins: effectors of morphogenesis. *Development* **126,** 2033–2044

45. Stein, E., Savaskan, N. E., Ninnemann, O., Nitsch, R., Zhou, R., and Skutella, T. (1999) A role for the Eph ligand ephrin-A3 in entorhino-hippocampal axon targeting. *J. Neurosci.* **19,** 8885–8893

46. Gao, P. P., Yue, Y., Cerretti, D. P., Dreyfus, C., and Zhou, R. (1999) Ephrin-dependent growth and pruning of hippocampal axons. *Proc. Natl. Acad. Sci. USA* **96,** 4073–4077

47. Raineteau, O., and Schwab, M. E. (2001) Plasticity of motor systems after incomplete spinal cord injury. *Nat. Rev. Neurosci.* **2,** 263–273

48. Witter, M. P., Groenewegen, H. J., Lopes-da-Silva, F. H., and Lohman, A. H. (1989) Functional organization of the extrinsic and intrinsic circuitry of the parahippocampal region. *Prog. Neurobiol.* **33,** 161–253

49. Bayer, S. A., and Altman, J. (1987) Directions in neurogenetic gradients and patterns of anatomical connections in the telencephalon. *Prog. Neurobiol.* **29,** 57–106

50. Braak, H., and Braak, E. (1991) Neuropathological stageing of Alzheimer-related changes. *Acta Neuropathol. (Berl.)* **82,** 239–259

51. Hyman, B. T., Van Horsen, G. W., Damasio, A. R., and Barnes, C. L. (1984) Alzheimer's disease: cell-specific pathology isolates the hippocampal formation. *Science* **225,** 1168–1170

52. Gall, C., Rose, G., and Lynch, G. (1979) Proliferative and migratory activity of glial cells in the partially deafferented hippocampus. *J. Comp. Neurol.* **183,** 539–549

53. Matthews, D. A., Cotman, C., and Lynch, G. (1976) An electron microscopic study of lesion-induced synaptogenesis in the dentate gyrus of the adult rat. I. Magnitude and time course of degeneration. *Brain Res.* **115,** 1–21

54. Matthews, D. A., Cotman, C., and Lynch, G. (1976) An electron microscopic study of lesion-induced synaptogenesis in the dentate gyrus of the adult rat. II. Reappearance of morphologically normal synaptic contacts. *Brain Res.* **115,** 23–41

55. Forster, E., Zhao, S., and Frotscher, M. (2001) Hyaluronan-associated adhesive cues control fiber segregation in the hippocampus. *Development* **128,** 3029–3039

56. Bovolenta, P., Fernaud-Espinosa, I., Mendez-Otero, R., and Nieto, S. (1997) Neurite outgrowth inhibitor of gliotic brain tissue. Mode of action and cellular localization, studied with specific monoclonal antibodies. *Eur. J. Neurosci.* **9,** 977–989

57. Deller, T., and Frotscher, M. (1997) Lesion-induced plasticity of central neurons: sprouting of single fibres in the rat hippocampus after unilateral entorhinal cortex lesion. *Prog. Neurobiol.* **53,** 687–727

58. Haas, C. A., Rauch, U., Thon, N., Merten, T., and Deller, T. (1999) Entorhinal cortex lesion in adult rats induces the expression of the neuronal chondroitin sulfate proteoglycan neurocan in reactive astrocytes. *J. Neurosci.* **19,** 9953–9963

59. Thon, N., Haas, C. A., Rauch, U., Merten, T., Fassler, R., Frotscher, M., and Deller, T. (2000) The chondroitin sulphate proteoglycan brevican is upregulated by astrocytes after entorhinal cortex lesions in adult rats. *Eur. J. Neurosci.* **12,** 2547–2558

60. Kovacs, A., Kwidzinski, E., Heimrich, B., and Nitsch, R. (2001) Transneuronal apoptosis following entorhinal cortex lesion in the dentate gyrus. *Soc. Neurosci. Abstr.* **27,** 253

61. Savaskan, N. E., Skutella, T., Brauer, A. U., Plaschke, M., Ninnemann, O., and Nitsch, R. (2000) Outgrowth-promoting molecules in the adult hippocampus after perforant path lesion. *Eur. J. Neurosci.* **12,** 1024–1032

62. Steward, O., Kelley, M. S., and Torre, E. R. (1993) The process of reinnervation in the dentate gyrus of adult rats: temporal relationship between changes in the levels of glial fibrillary acidic protein (GFAP) and GFAP mRNA in reactive astrocytes. *Exp. Neurol.* **124,** 167–183

63. Cotman, C. W., and Nieto-Sampedro, M. (1985) Progress in facilitating the recovery of function after central nervous system trauma. *Ann. N. Y. Acad. Sci.* **457,** 83–104

64. Deller, T., Frotscher, M., and Nitsch, R. (1995) Morphological evidence for the sprouting of inhibitory commissural fibers in response to the lesion of the excitatory entorhinal input to the rat dentate gyrus. *J. Neurosci.* **15,** 6868–6878

65. Cadelli, D. S., Bandtlow, C. E., and Schwab, M. E. (1992) Oligodendrocyte- and myelin-associated inhibitors of neurite outgrowth: their involvement in the lack of CNS regeneration. *Exp. Neurol.* **115,** 189–192

66. Wang, K. C., Koprivica, V., Kim, J. A., Sivasankaran, R., Guo, Y., Neve, R. L., and He, Z. (2002) Oligodendrocyte-myelin glycoprotein is a Nogo receptor ligand that inhibits neurite outgrowth. *Nature (London)* **417,** 941–944

67. Bendotti, C., Baldessari, S., Pende, M., Southgate, T., Guglielmetti, F., and Samanin, R. (1997) Relationship between GAP-43 expression in the dentate gyrus and synaptic reorganization of hippocampal mossy fibres in rats treated with kainic acid. *Eur. J. Neurosci.* **9,** 93–101

68. Schnell, L., Schneider, R., Kolbeck, R., Barde, Y. A., and Schwab, M. E. (1994) Neurotrophin-3 enhances sprouting of corticospinal tract during development and after adult spinal cord lesion. *Nature (London)* **367,** 170–173

69. Weibel, D., Cadelli, D., and Schwab, M. E. (1994) Regeneration of lesioned rat optic nerve fibers is improved after neutralization of myelin-associated neurite growth inhibitors. *Brain Res.* **642,** 259–266

70. Van de Velde, H. J., Roebroek, A. J., Senden, N. H., Ramaekers, F. C., and Van de Ven, W. J. (1994) NSP-encoded reticulons, neuroendocrine proteins of a novel gene family associated with membranes of the endoplasmic reticulum. *J. Cell Sci.* **107,** 2403–2416

71. Alcantara, S., Ruiz, M., De Castro, F., Soriano, E., and Sotelo, C. (2000) Netrin 1 acts as an attractive or as a repulsive cue for distinct migrating neurons during the development of the cerebellar system. *Development* **127,** 1359–1372

72. Wu, W., Wong, K., Chen, J., Jiang, Z., Dupuis, S., Wu, J. Y., and Rao, Y. (1999) Directional guidance of neuronal migration in the olfactory system by the protein Slit. *Nature (London)* **400,** 331–336

73. Baka, I. D., Ninkina, N. N., Pinon, L. G., Adu, J., Davies, A. M., Georgiev, G.-P., and Buchman, V. L. (1996) Intracellular compartmentalization of two differentially spliced s-rex/NSP mRNAs in neurons. *Mol. Cell. Neurosci.* **7,** 289–303

74. Hens, J., Nuydens, R., Geerts, H., Senden, N. H., Van de Ven, W. J., Roebroek, A. J., van de Velde, H. J., Ramaekers, F. C., and Broers, J. L. (1998) Neuronal differentiation is accompanied by NSP-C expression. *Cell Tissue Res.* **292,** 229–237

75. Hu, W. H., Hausmann, O. N., Yan, M. S., Walters, W. M., Wong, P. K., and Bethea, J. R. (2002) Identification and characterization of a novel Nogo-interacting mitochondrial protein (NIMP). *J. Neurochem.* **81,** 36–45

76. Liu, B. P., Fournier, A., GrandPre, T., and Strittmatter, S. M. (2002) Myelin-associated glycoprotein as a functional ligand for the Nogo-66 receptor. *Science online Jun 27*.

77. Wang, K. C., Kim, J. A., Sivasankaran, R., Segal, R., and He, Z. (2002) P75 interacts with the Nogo receptor as a co-receptor for Nogo, MAG and OMgp. *Nature (London)* **420,** 74–78

78. Tessier-Lavigne, M., and Goodman, C. S. (2000) Perspectives: neurobiology. Regeneration in the Nogo zone. *Science* **287,** 813–814

79. Brittis, P. A., and Flanagan, J. G. (2001) Nogo domains and a Nogo receptor: implications for axon regeneration. *Neuron* **30,** 11–14

80. Steup, A., Ninnemann, O., Savaskan, N. E., Nitsch, R., Puschel, A. W., and Skutella, T. (1999) Semaphorin D acts as a repulsive factor for entorhinal and hippocampal neurons. *Eur. J. Neurosci.* **11,** 729–734

81. Steup, A., Lohrum, M., Hamscho, N., Savaskan, N. E., Ninnemann, O., Nitsch, R., Fujisawa, H., Puschel, A. W., and Skutella, T. (2000) Sema3C and netrin-1 differentially affect axon growth in the hippocampal formation. *Mol. Cell. Neurosci.* **15,** 141–155

82. Wang, X., Chun, S. J., Treloar, H., Vartanian, T., Greer, C. A., and Strittmatter, S. M. (2002) Localization of Nogo-A and Nogo-66 receptor proteins at sites of axon-myelin and synaptic contact. *J. Neurosci.* **22,** 5505–5515

83. Z'Graggen, W. J., Metz, G. A., Kartje, G. L., Thallmair, M., and Schwab, M. E. (1998) Functional recovery and enhanced corticofugal plasticity after unilateral pyramidal tract lesion and blockade of myelin-associated neurite growth inhibitors in adult rats. *J. Neurosci.* **18,** 4744–4757

Received August 14, 2002; accepted February 12, 2003.

Fig. 1

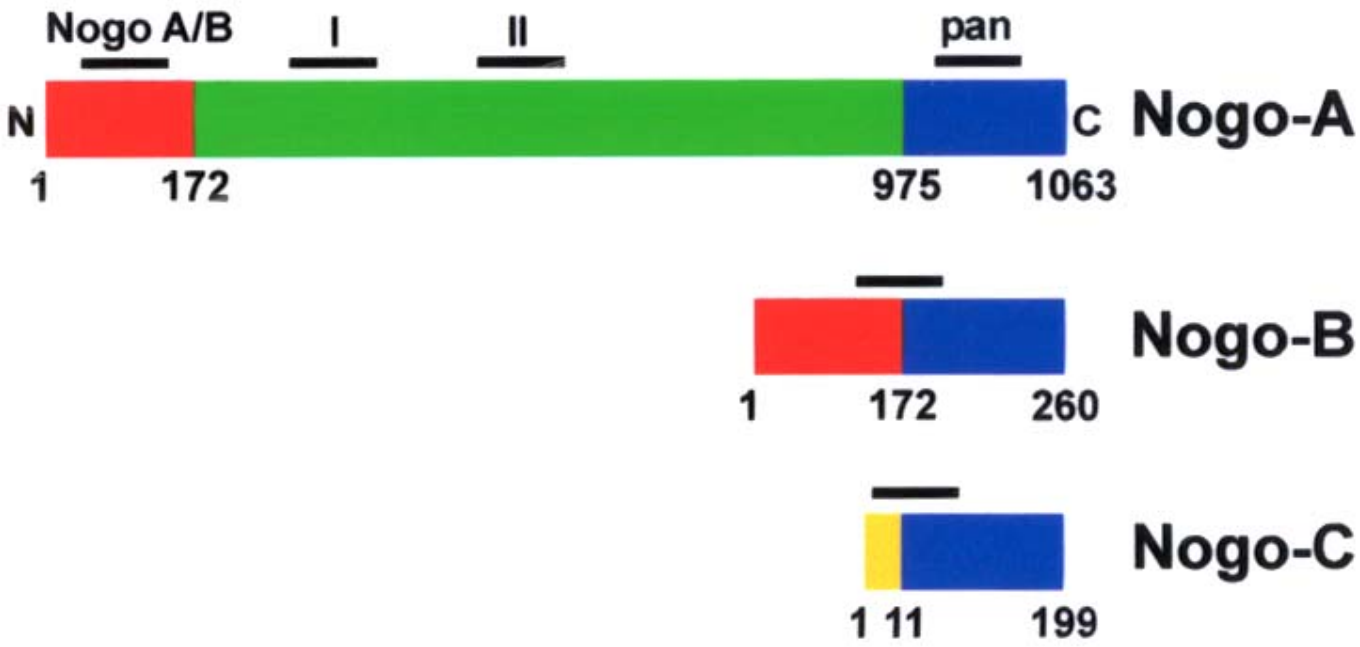

Figure 1. Schematic of Nogo genes and indicated probe regions. Three different isoforms, the 4.6-kb-long transcript Nogo-A, the 2.6-kb-long Nogo-B, and the 1.7-kb-long Nogo-C are generated by alternative promoter usage and/or splicing from a single gene. The oligonucleotide Nogo-A/B is specific for the splice forms Nogo-A and Nogo-B, whereas the oligonucleotide Nogo pan detects all three Nogo forms (blue region) because of the common 188 amino acid long C terminus. The Nogo-A I, Nogo-A II, Nogo-A/B, and Nogo-A pan oligonucleotides essentially gave the same expression pattern as the Nogo-A-specific oligonucleotides alone. The oligonucleotides Nogo-A I, Nogo-A II, Nogo-B, and Nogo-C were specific for the respective genes. The red region indicates sequence homology of Nogo-A and Nogo-B; the green region indicates unique sequence of Nogo-A; the yellow region indicates the unique 150 bp of Nogo-C mRNA.

Fig. 2

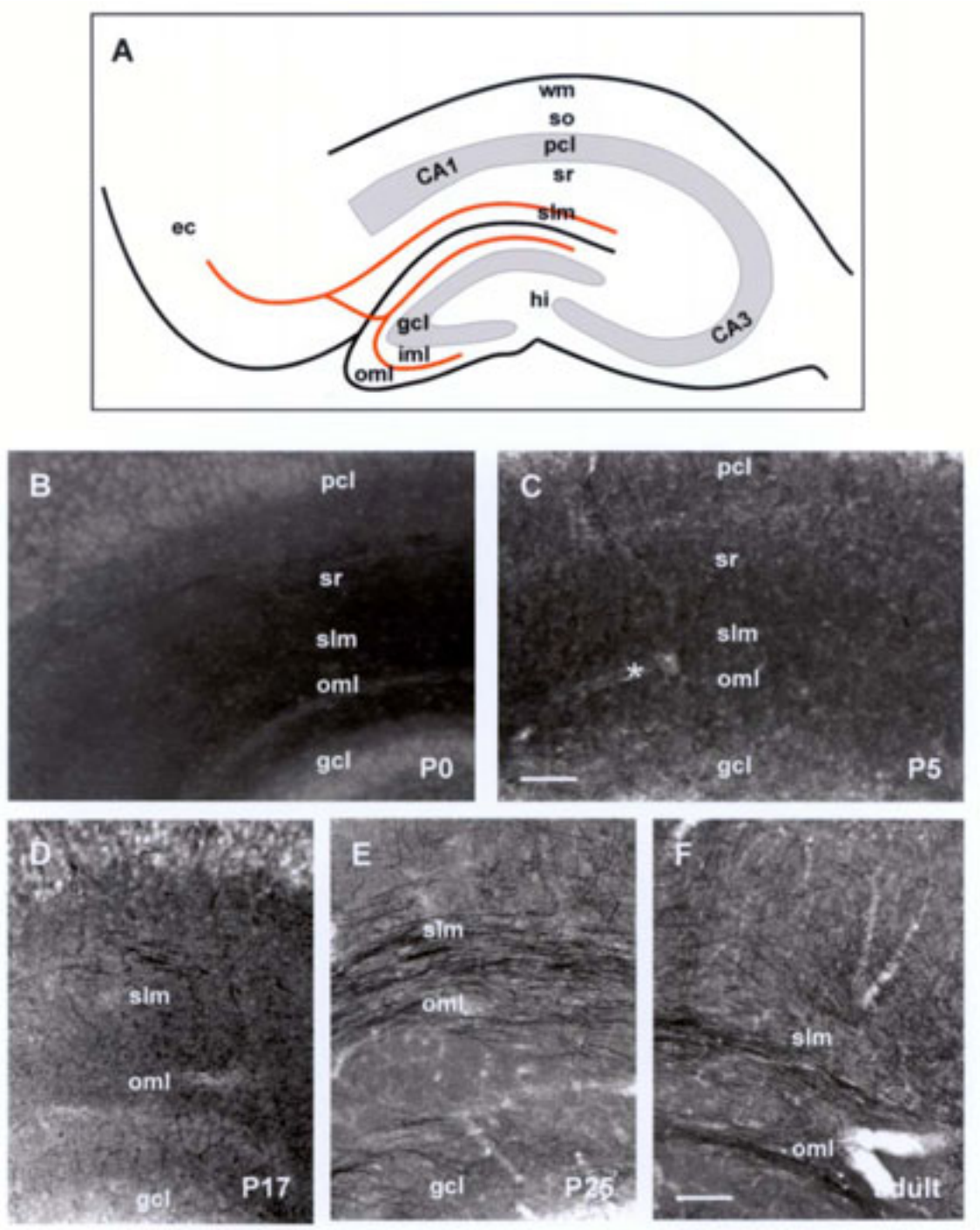

Figure 2. Myelination of the hippocampus during development. ***A*****)** Schematic diagram of the lamination and main projection to the hippocampus. The perforant path originates from the layer II and layer III neurons of the entorhinal cortex (ec) and terminates in the outer molecular layer (oml) of the dentate gyrus and in the stratum lacunosum-moleculare (slm) of the CA1-CA3 region. iml, inner molecular layer of the dentate gyrus; hi, hilus; CA, cornu ammonis; sr, stratum radiata; so, stratum oriens; wm, white matter; pcl, pyramidal cell layer; gcl, granule cell layer. ***B–F*****)** Myelinated fiber detection revealed by Black Gold staining in the developing hippocampal region. The first appearance of myelinated fibers in the hippocampus was seen at postnatal day 17 (P17) in the outer molecular layer (oml) of the dentate gyrus and in the stratum lacunosum-moleculare (slm) (***D***), whereas at P0 and P5 hardly any Black Gold stained fibers were detectable (***B***, ***C***). The myelination pattern in the entorhinal termination zone was fulfilled at P25 and remained unchanged throughout adulthood (***E***, ***F***). Scale bar for ***B*** and ***C*** = 100 μm; scale bar in ***F*** for ***D***, ***E***, and ***F*** = 60 μm. The asterisk in ***C*** indicates a blood vessel.

Fig. 3

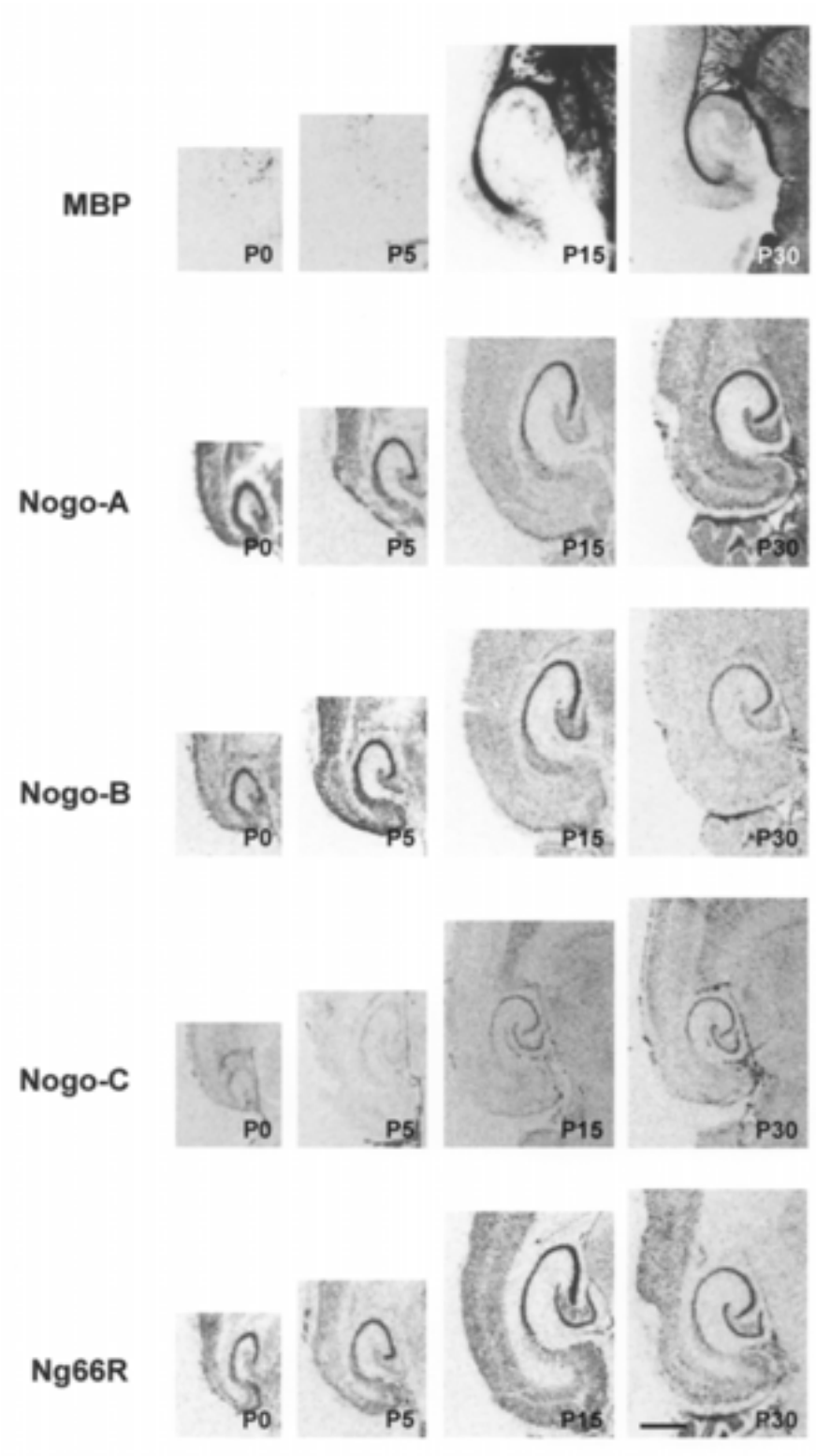

Figure 3. Expression of Nogo genes and MBP in the developing hippocampus: in situ hybridization of horizontal hippocampal sections of different developmental time points. At P0, Nogo-A and Nogo-B and Ng66R transcripts were located in the hippocampal subregions, whereas the Nogo-C mRNA appeared in a significant amount first at P15. At P30, all three Nogo transcripts and the receptor were present in the hippocampus, with the strongest hybridization signals for Nogo-A. In contrast, MBP mRNA first appeared at P15 in the hippocampal neurophil, whereas neuronal cell layers were devoid of hybridization signals. At P30, MBP transcripts were located in the strata lacunosum-moleculare and oriens, with the strongest signals in the fimbria and anterior commissure. Scale bar = 900 μm.

Fig. 4

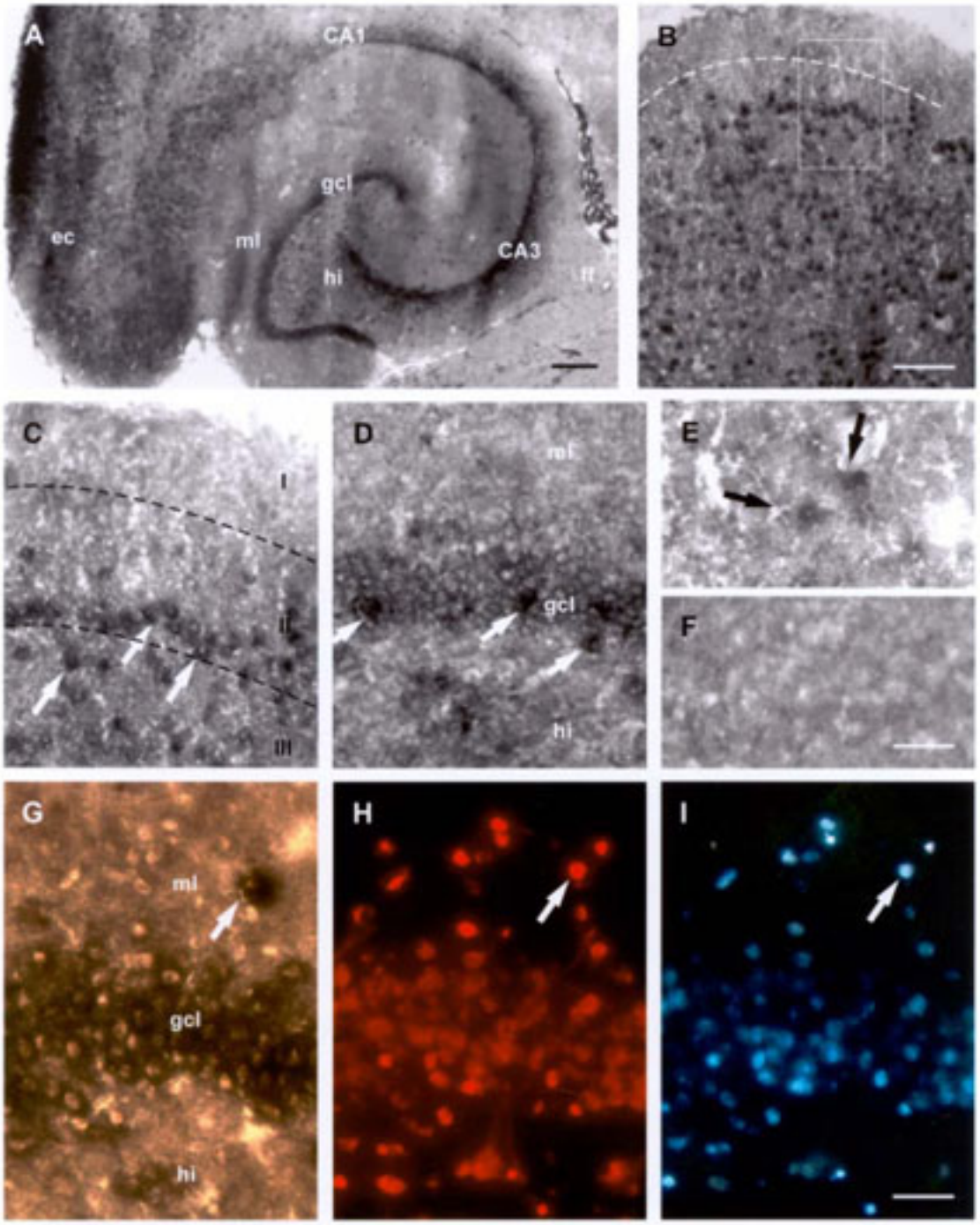

Figure 4. Cellular distribution of Nogo-A mRNA expression in the adult hippocampus. ***A*****)** Overview shows the nonradioactive hybridization pattern of Nogo-A transcripts in the hippocampal formation. gcl, granule cell layer; ml, molecular layer; CA, cornu ammonis; hi, hilus; ff, fimbria fornix. ***B*****)** Nogo-A-expressing neurons were observed in the entorhinal cortex (ec) of layers II and III, whereas layer I was devoid of any hybridization signal. ***C*****)** Higher magnification of the boxed area in ***B***. Arrows indicate strongly labeled neurons in layers II and III. ***D*****)** Nogo-A mRNA-positive neurons were found in the granule cell layer of the dentate gyrus, whereas the molecular layer was free of any hybridization signal. ***E*****)** Higher magnification of the fimbria fornix in ***A***. In the white matter, Nogo-A mRNA was found in oligodendrocytes (arrows). ***F*****)** Note the absence of staining in the controls, which were hybridized with the sense probe. Nogo-A mRNA-expressing cells in the dentate gyrus (***G***) and the corresponding Nissl staining (***H***) and nuclear staining (***I***). Scale bar in ***A*** = 200 μm; in ***B*** = 40 μm; in ***F*** for ***C***, ***D***, ***E***, and ***F*** = 35 μm; in ***I*** for ***G***, ***H***, and ***I*** = 20 μm.

Fig. 5

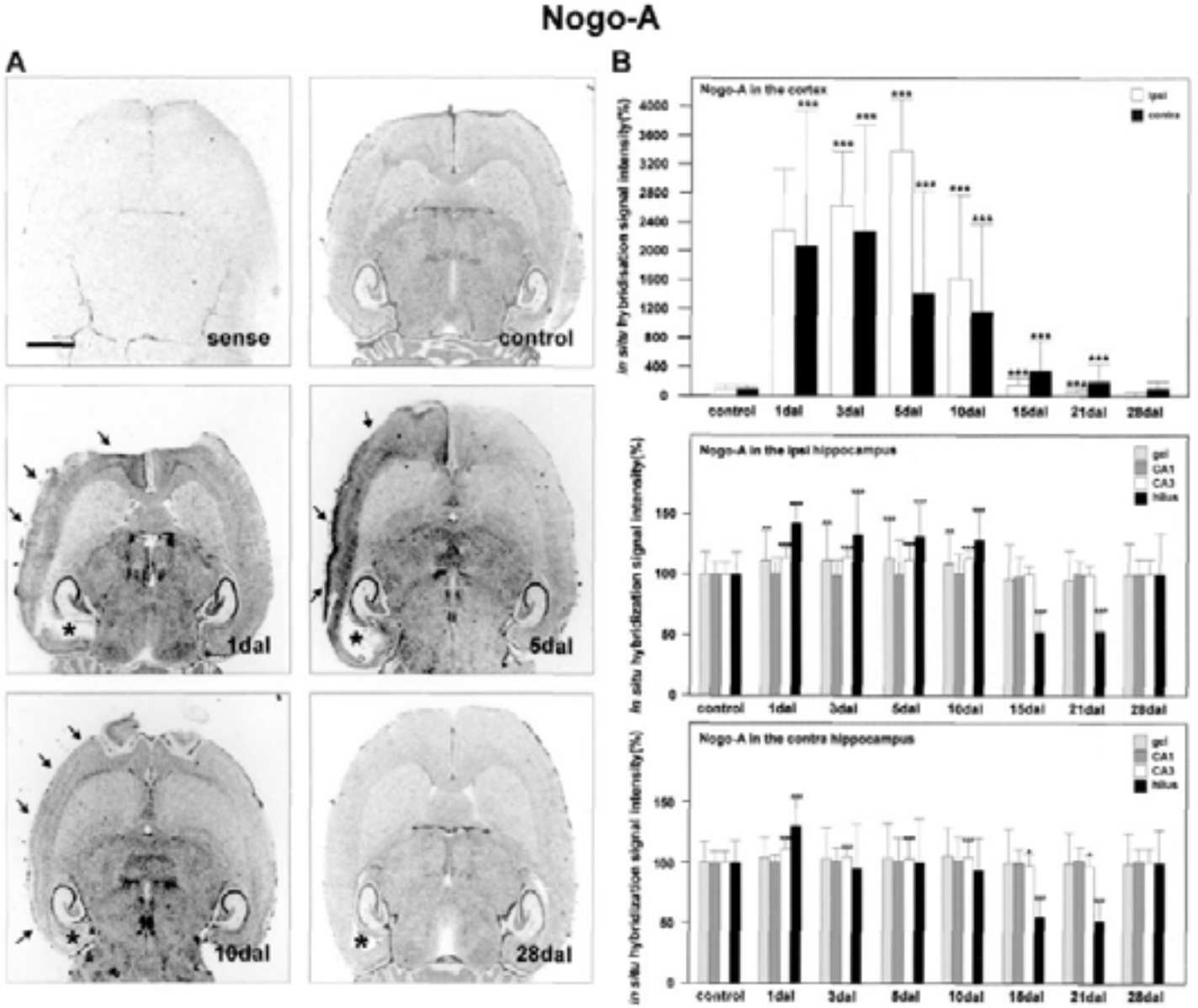

Figure 5. Expression pattern and quantitative analysis of Nogo-A mRNA after lesion in rat brain. ***A)*** Expression of Nogo-A transcripts in horizontal brain sections of adult nonlesioned controls, 1 day after lesion (dal), 5 dal, 10 dal, and 28 dal, as detected by in situ hybridization with Nogo-A I oligonucleotide. Arrows indicate areas of expression alterations after ECL in the cortex. Strong upregulation in CA1, CA3, dentate gyrus, and hilar region was already detectable at 1 dal. At 10 dal, mRNA expression levels of the CA region reached control levels, whereas the hilar region showed decreased hybridization signals in comparison to nonlesioned controls. The sense image shows a brain section probed with an excess of unlabeled oligonucleotides. Asterisks point to the lesion side. Scale bar = 3.75 mm. ***B)*** Quantitative analysis of Nogo-A mRNA expression in the cortex and hippocampus of both sides of the lesion. The time course of changes in mRNA expression after ECL was analyzed by in situ hybridization in the cortex, granule cell layer (gcl), CA1, CA3, and hilar region. Data are expressed as the percentage of means of the optical density found in the adult nonlesioned controls. Results are given ± SD for 6 rats in each group ($n = 12$). Statistical significance is indicated by asterisks (*$P<0.05$; **$P<0.01$; ***$P<0.001$; Mann-Whitney U test).

Fig. 6

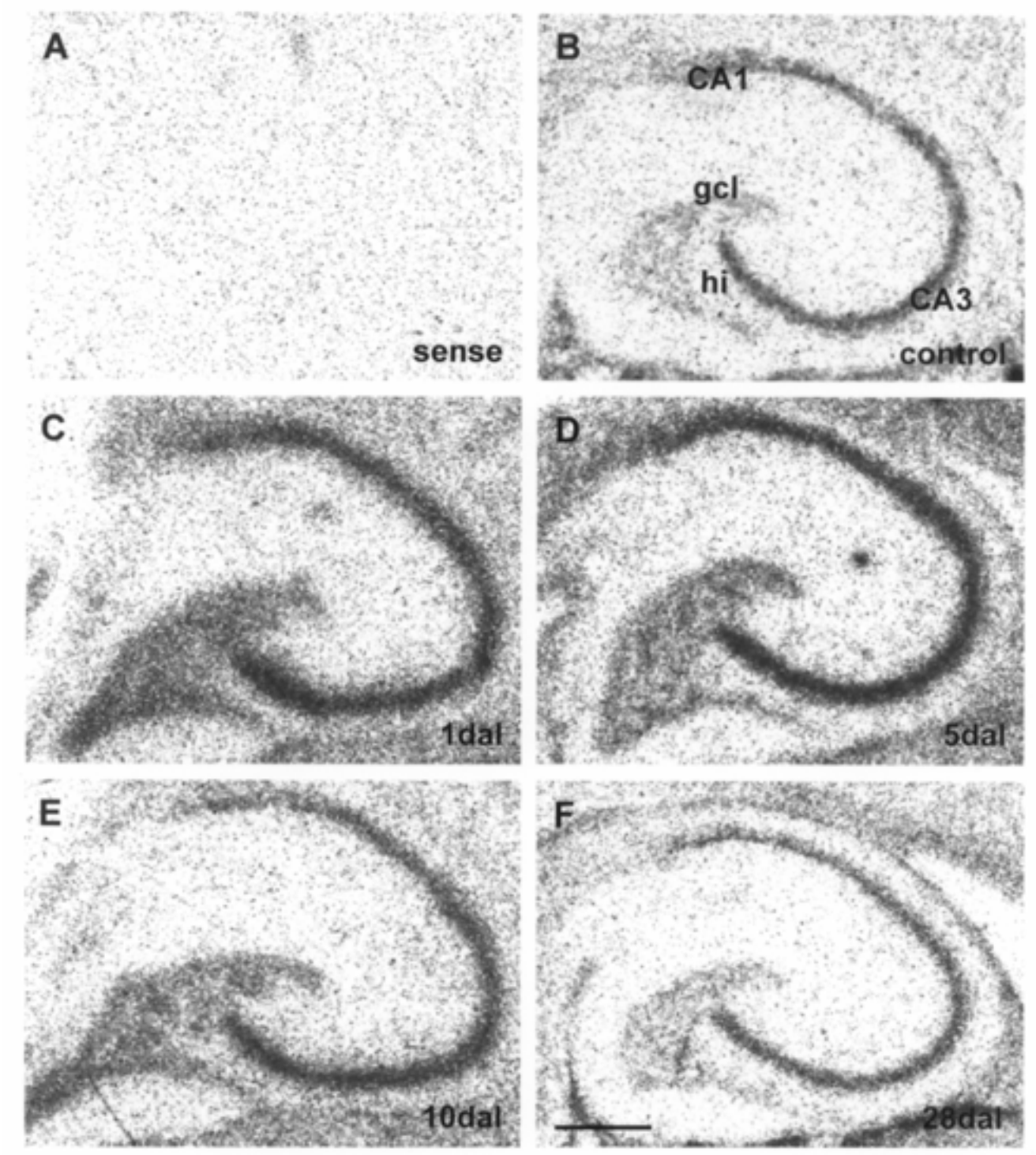

Figure 6. Nogo-A mRNA expression pattern in the hippocampus after lesion. ***A*****)** The sense image shows a brain section probed with an excess of unlabeled oligonucleotides. Expression of Nogo-A mRNA hybridization pattern in horizontal brain sections of adult nonlesioned controls (***B***), and 1 (***C***), 5 (***D***), 10 (***E***), and 28 (***F***) dal as detected by in situ hybridization with the Nogo-A I oligonucleotide. Strong upregulation in the CA1, CA3, dentate gyrus, and hilar (hi) region was already detectable at 1 dal. At 10 dal, the mRNA expression levels of the CA region reached control levels, whereas the hilar regions showed decreased hybridization signals in comparison to nonlesioned controls. Scale bar = 400 μm. gcl, granule cell layer; CA, cornu ammonis.

Fig. 7

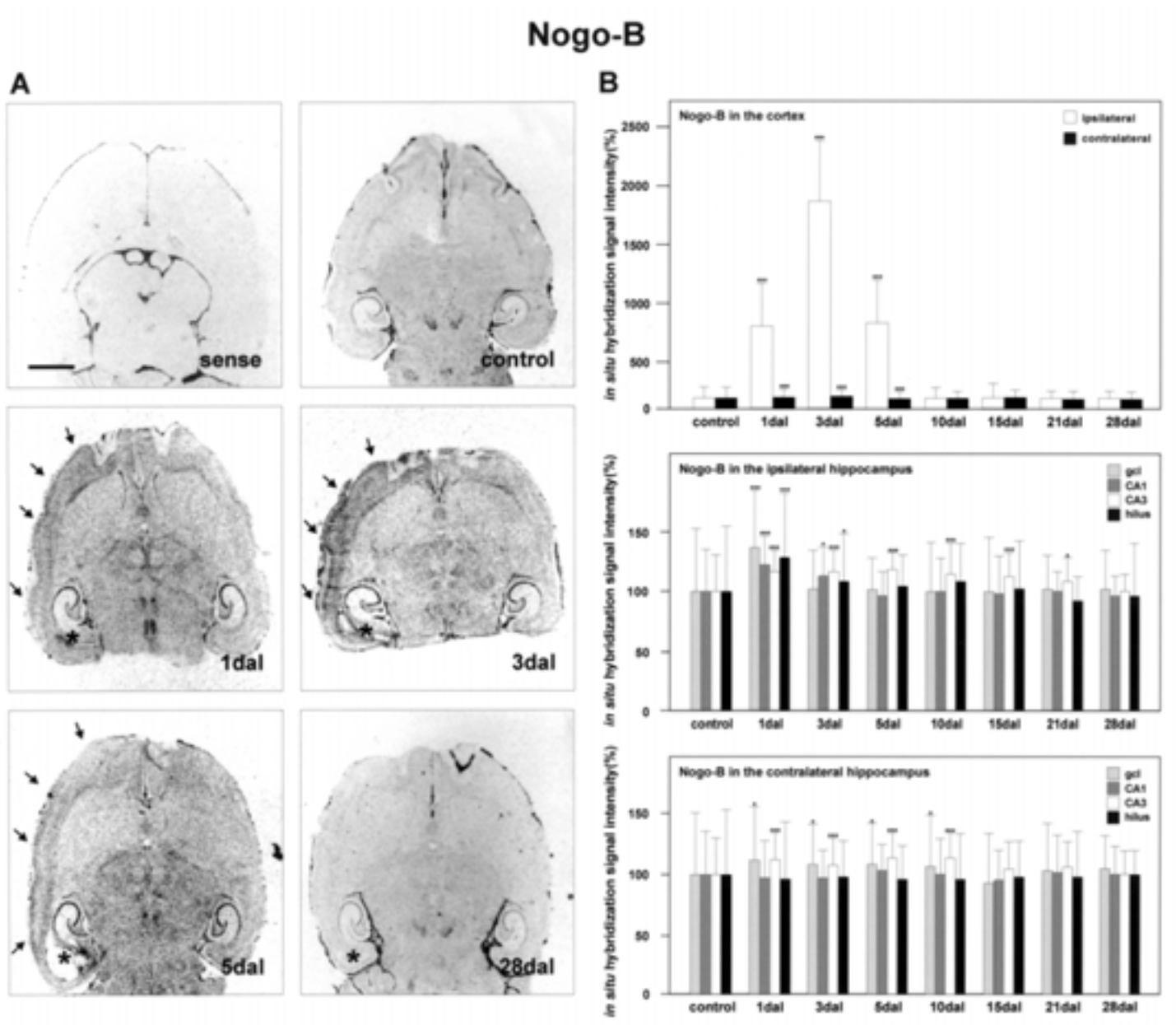

Figure 7. Nogo-B mRNA expression pattern and quantitative analysis after lesion in rat brain. ***A***) Nogo-B mRNA hybridization pattern in the adult rat brain, 1, 3, 5, and 28 dal as detected by in situ hybridization with the Nogo-B oligonucleotide. The sense image shows an adult rat brain section hybridized with a 100-fold surplus of unlabeled oligonucleotides. Arrows indicate strong upregulation in ipsilateral cortex at 1 dal until 5 dal. At 1 dal, an increased hybridization pattern in all cell layers of the ipsilateral hippocampus occurred, which was subsequently reduced in longer survival stages. Asterisks indicate the lesion side. Scale bar = 3.75 mm. ***B***) Quantitative analysis of Nogo-B mRNA expression in the cortex and hippocampus of both sides of the lesion. The time course of changes in mRNA expression after ECL was analyzed by in situ hybridization in the granule cell layer (gcl), CA1, CA3, and hilar region. Data are expressed as the percentage of means of the optical density found in the adult nonlesioned controls. Results are given ± SD from 6 rats in each group (n = 12). Statistical significance is indicated by asterisks (*P<0.05; **P<0.01; ***P<0.001; Mann-Whitney U test).

Fig. 8

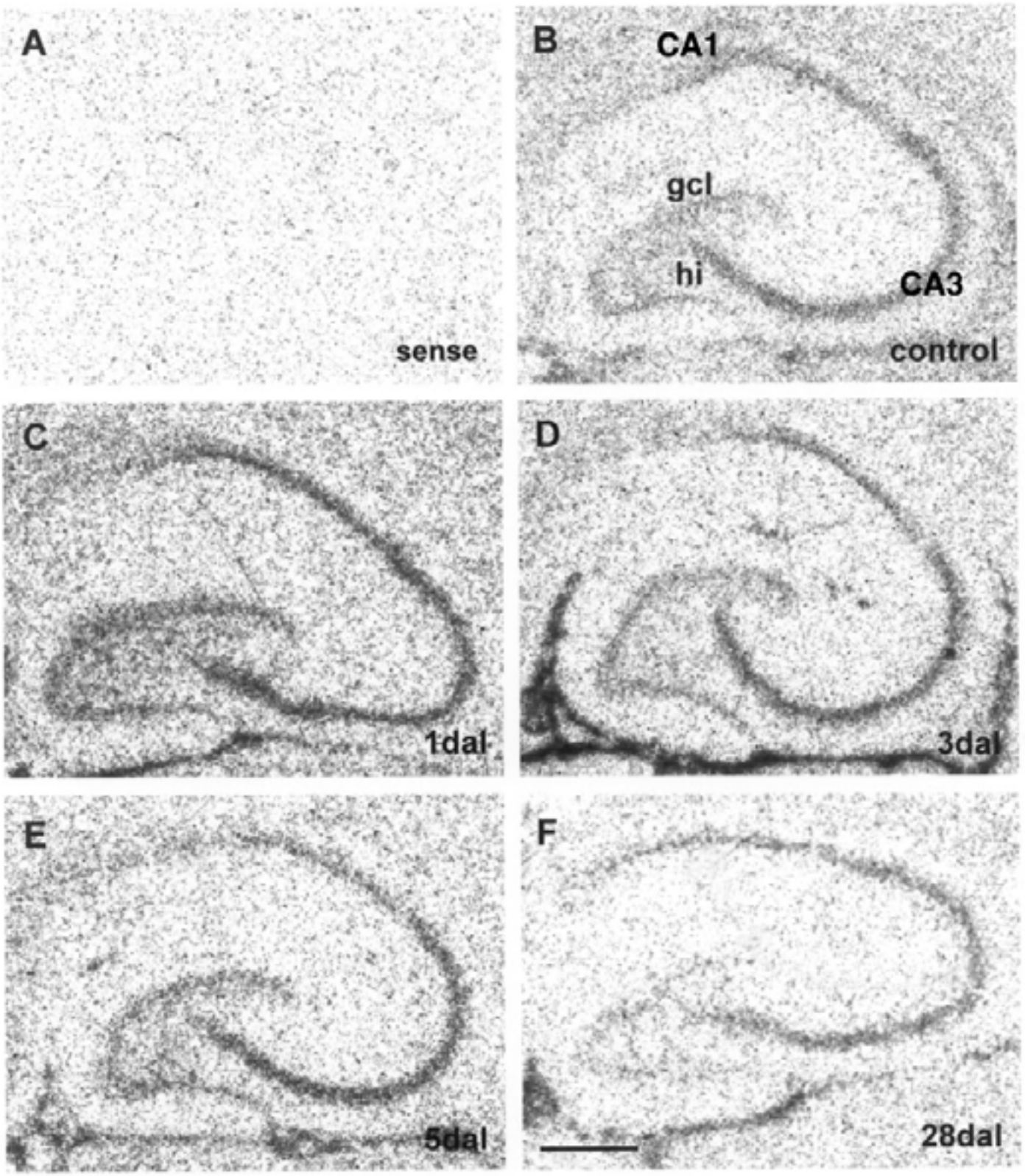

Figure 8. Nogo-B mRNA expression pattern in the hippocampus after lesion. *A*) The sense image shows a brain section probed with an excess of unlabeled oligonucleotides. Nogo-B mRNA hybridization pattern in the adult rat brain controls (***B***), and 1 (***C***), 3 (***D***), 5 (***E***), and 28 (***F***) dal as detected by in situ hybridization with the Nogo-B oligonucleotide. Scale bar = 400 μm. gcl, granule cell layer; hi, hilus; CA, cornu ammonis.

Fig. 9

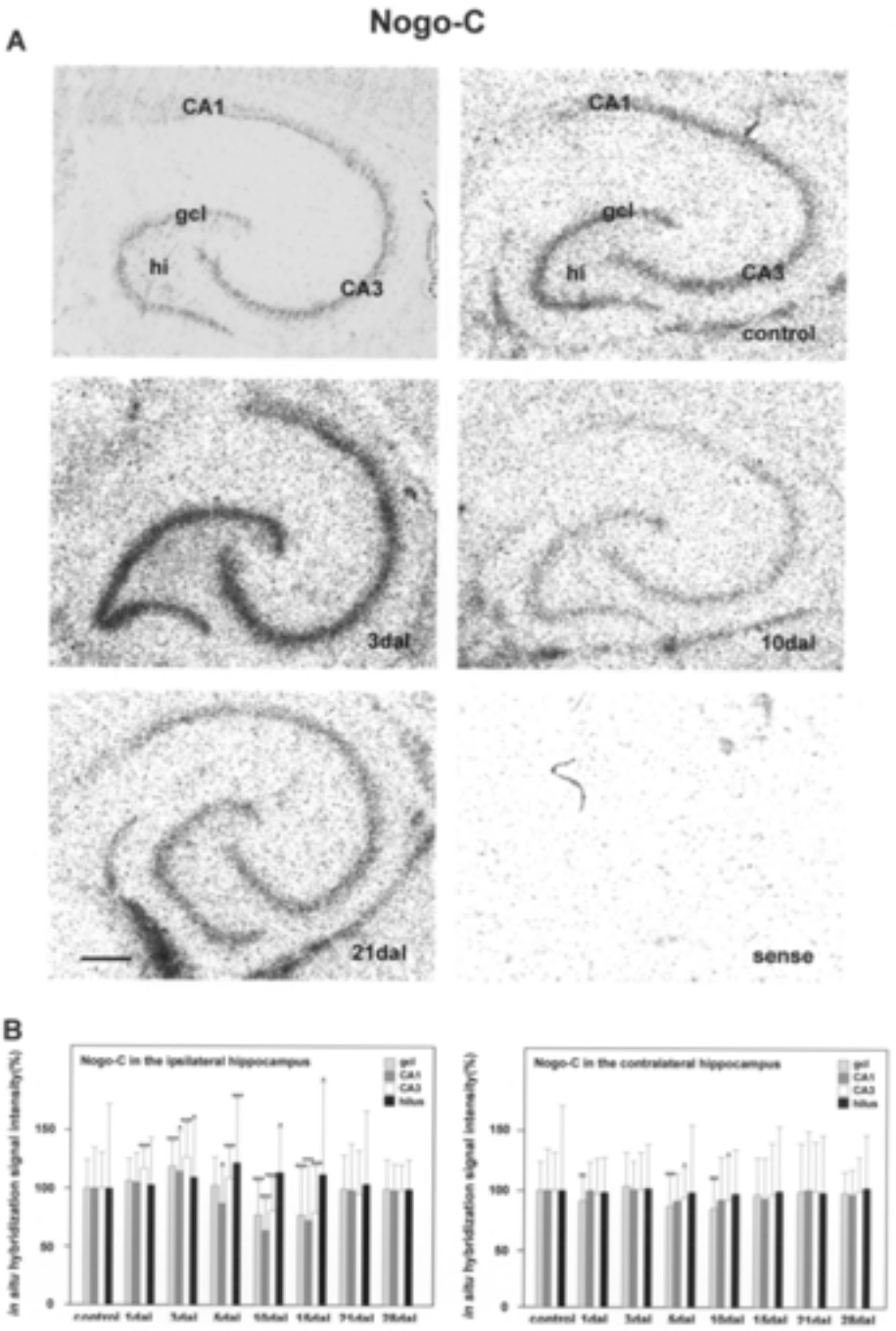

Figure 9. Expression pattern and quantitative analysis of Nogo-C mRNA after lesion in rat hippocampus. ***A***) In situ hybridization analysis of Nogo-C transcripts in horizontal sections of adult control hippocampus, 1, 3, 5, 10, 15, and 21 dal and the corresponding Nissl-stained sections. A strong increase in hybridization signal was detectable in all cell layers of the ipsilateral hippocampus at 1 and 3 dal. At 5 dal, a reduced signal was detected specifically in the CA1 region. A strong decrease in Nogo-C mRNA levels occurred in the CA1-CA3 region and in the granule cell layer (gcl) at 10 and 15 dal, whereas the signal in the hilus (hi) remained up-regulated. The hybridization signal reverted to basal level at 21 dal. Adult rat brain sections hybridized with a 100-fold surplus of unlabeled oligonucleotides served as controls. CA, cornu ammonis. Scale bar = 400 μm. ***B***) Quantitative analysis of Nogo-C mRNA expression in the cortex and hippocampus of both sides of the lesion. The time course of changes in mRNA expression after ECL was analyzed by in situ hybridization in the granule cell layer (gcl), CA1, CA3, and hilar region. Data are expressed as the percentage of means of the optical density found in the adult nonlesioned controls. Results are given ± SD from 6 rats in each group (n = 12). Statistical significance is indicated by asterisks (*P<0.05; **P<0.01; ***P<0.001; Mann-Whitney U test).

Fig. 10

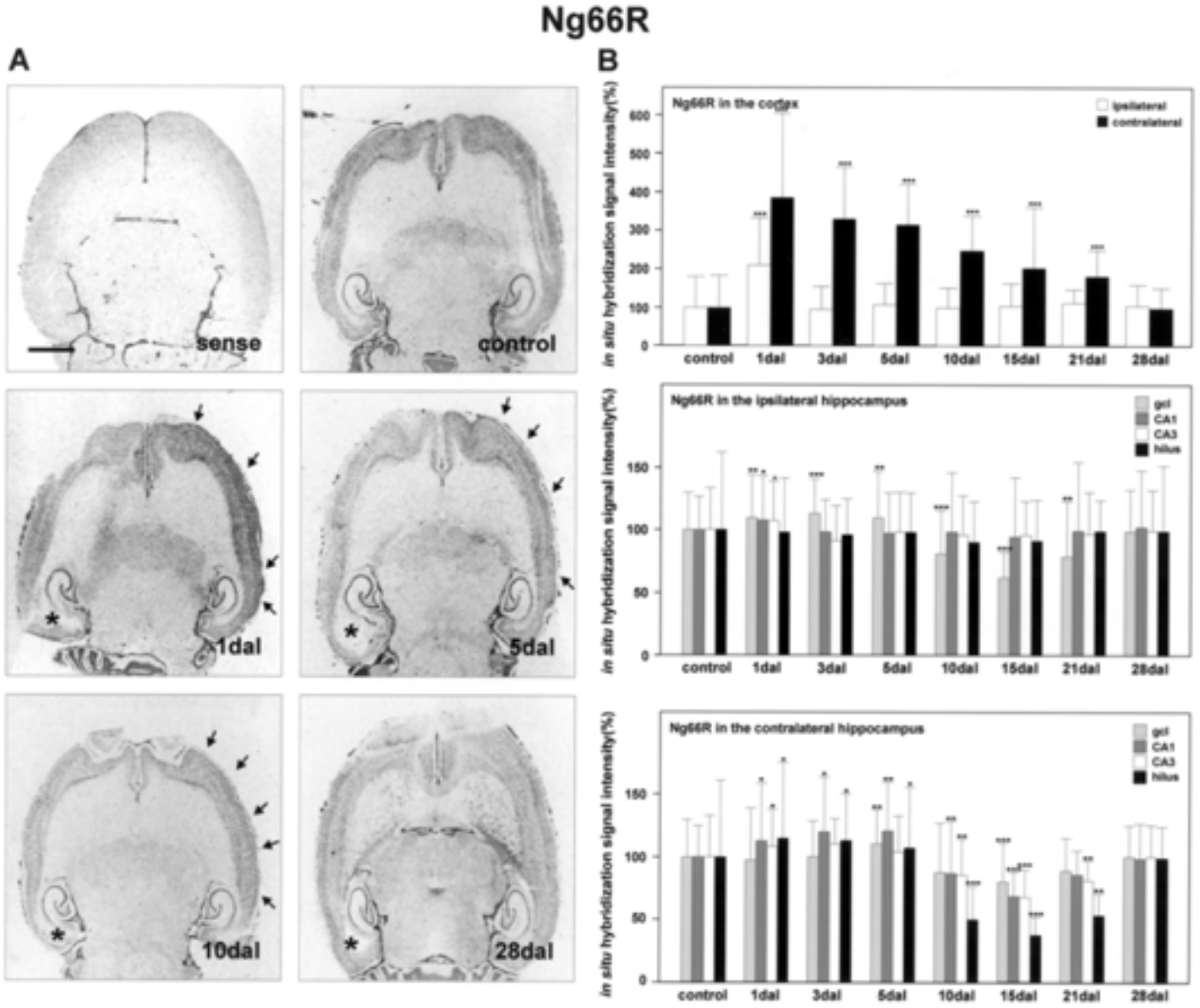

Figure 10. Ng66R mRNA expression pattern and quantitative analysis after lesion. ***A*)** Hybridization signal of Ng66R mRNA in horizontal adult brain sections from nonlesioned controls, and 1, 5, 10, and 28 dal. Arrows indicate the increased hybridization signals in the contralateral cortex. Asterisks indicate the lesion side. Controls were obtained with a 100-fold surplus of unlabeled oligonucleotides. Scale bar = 3.75 mm. ***B*)** Quantitative analysis of the Ng66R expression in the cortex, granule cell layer of the dentate gyrus, pyramidal cells of the CA1 and CA3 region, and hilar region of both sides of the lesion. Data are expressed as the percentage of means of the optical density found in the adult nonlesioned controls. Results are given ± SD from 6 rats in each group ($n = 12$). Statistical significance is indicated by asterisks (*P<0.05; **P<0.01; ***P<0.001; Mann-Whitney U test).

Fig. 11

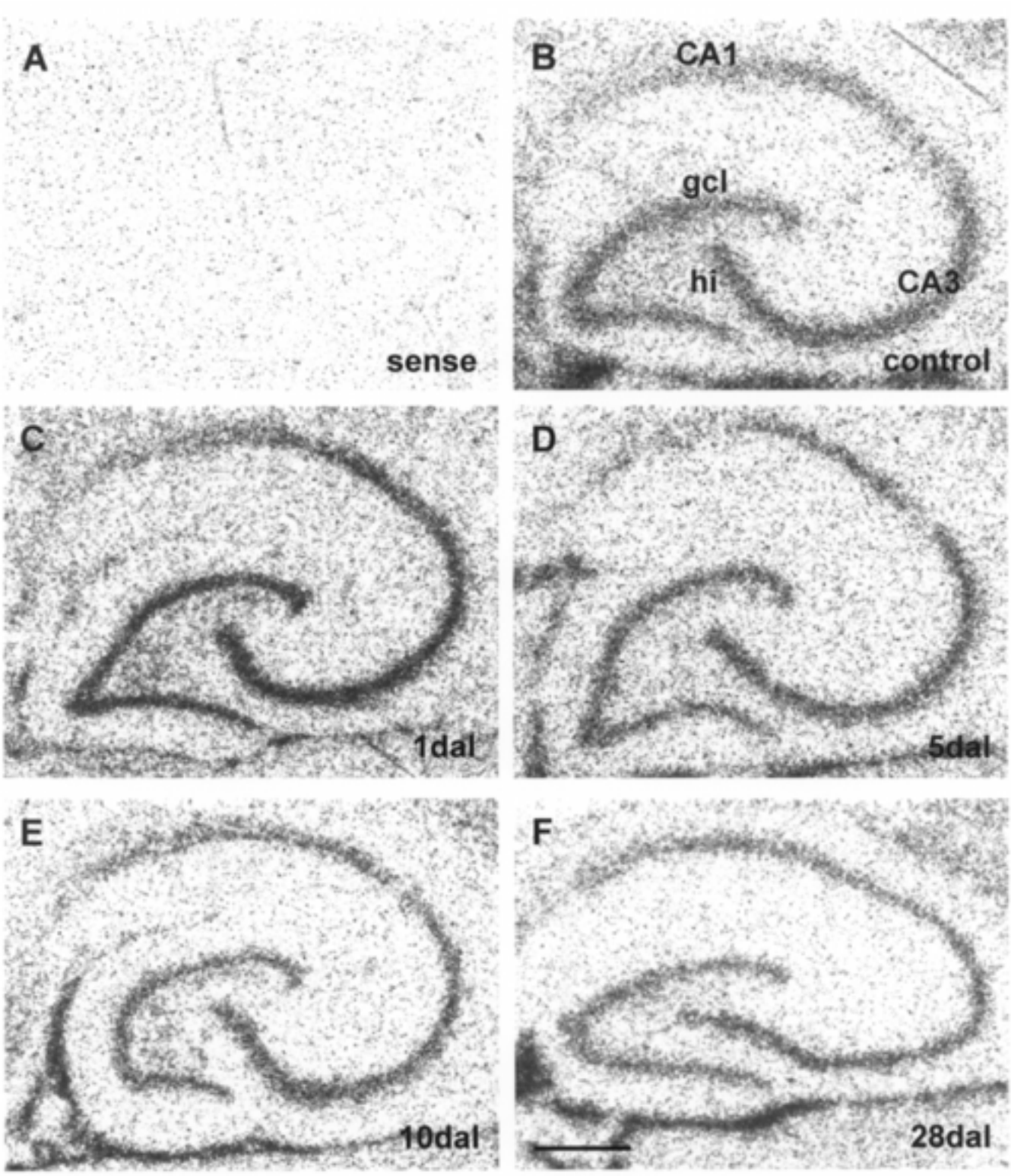

Figure 11. Ng66R mRNA expression pattern in the hippocampus after lesion. ***A*****)** The sense image shows a brain section probed with an excess of unlabeled oligonucleotides. Ng66R mRNA expression in horizontal adult brain sections from nonlesioned controls (***B***), and 1 (***C***), 5 (***D***), 10 (***E***), and 28 (***F***) dal. Scale bar = 400 μm. gcl, granule cell layer; hi, hilus; CA, cornu ammonis.

Fig. 12

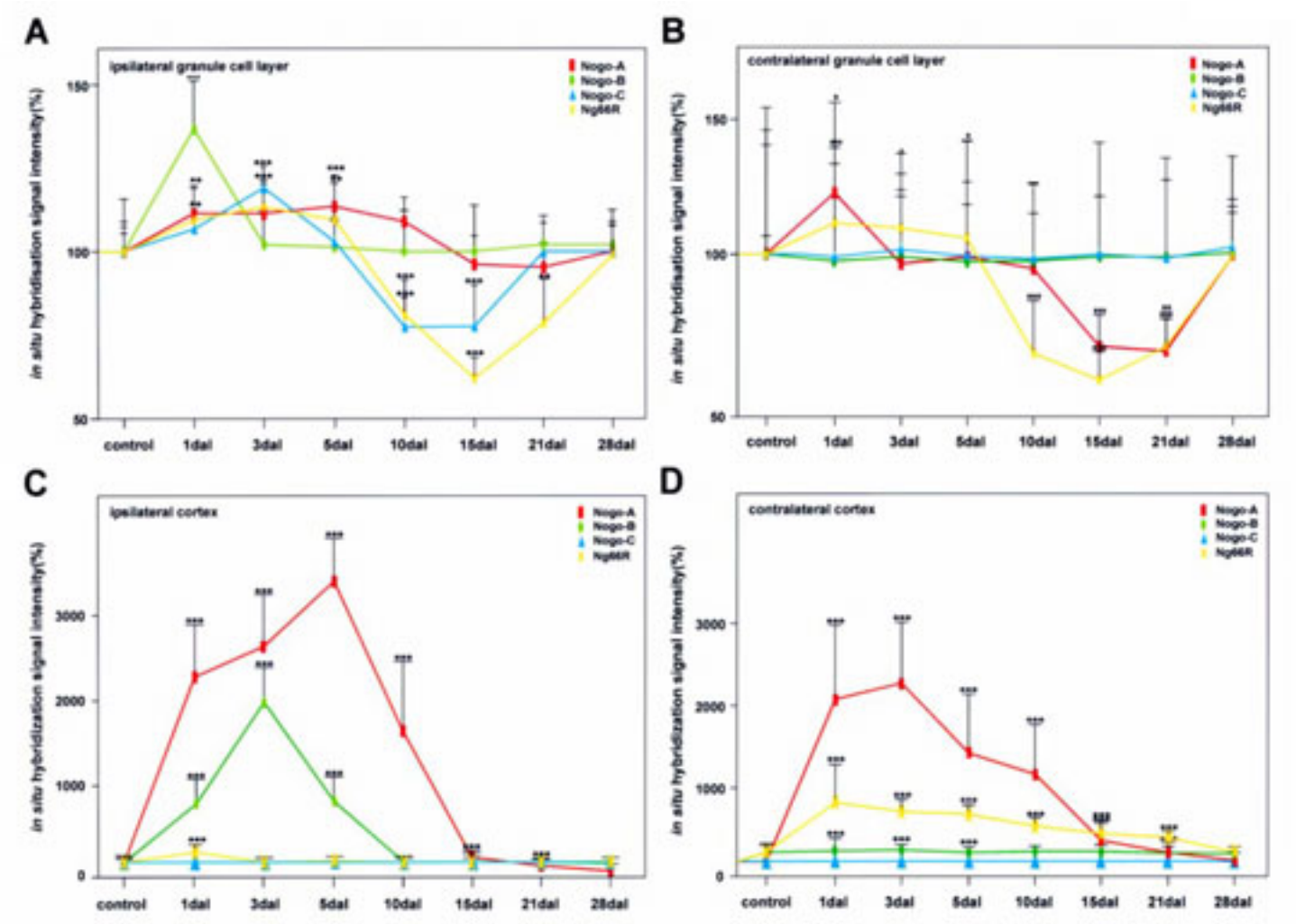

Figure 12. Longitudinal expression profile of Nogo genes in the hippocampus after entorhinal lesion. Values of relative levels of Nogo-A, -B, and -C and Ng66R mRNAs from in situ hybridization analysis are given for adult nonlesioned controls and 1–28 dal in ipsilateral and contralateral granule cell layers of the dentate gyrus (***A***, ***B***) and ipsilateral and contralateral cortex (***C***, ***D***). Results are given ± SD from 6 rats in each group ($n = 12$). Statistical significance is indicated by asterisks (*P<0.05; **P<0.01; ***P<0.001; Mann-Whitney U test).

Fig. 13

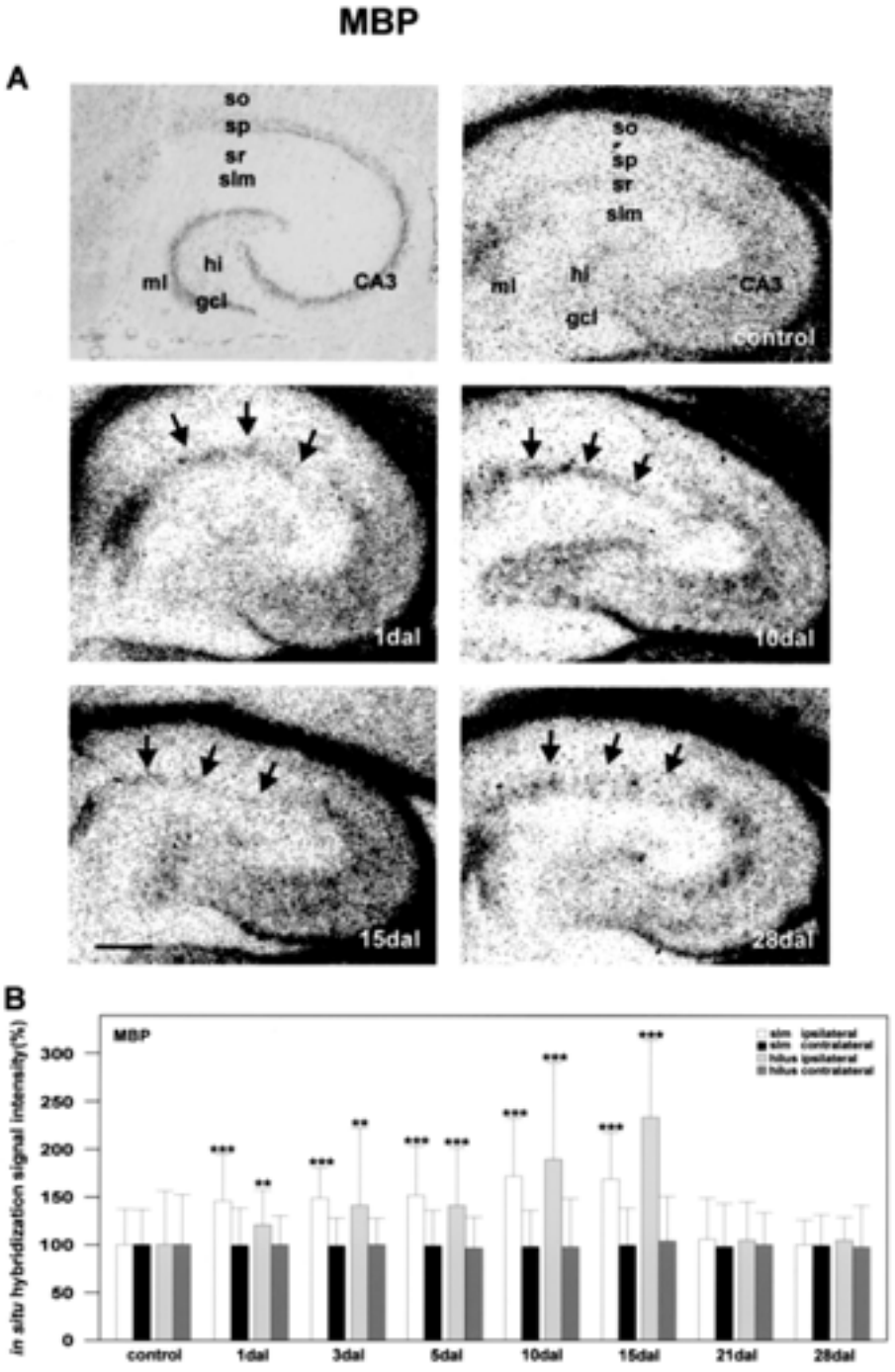

Figure 13. MBP mRNA expression pattern and quantitative analysis after lesion in the hippocampus. *A*) Expression of MBP mRNA in horizontal sections of adult control hippocampus 1, 10, 15, and 28 dal and the corresponding Nissl-stained section. Increased expression signals were present in the strata lacunosum-moleculare (slm) and radiata (sr) of the CA3 region and the hilar (hi) region with a maximum at 15 dal. Controls were obtained with a 100-fold surplus of unlabeled oligonucleotides. CA, cornu ammonis; gcl, granule cell layer; ml, molecular layer; so, stratum oriens; sr, stratum radiatum. Scale bar = 360 μm. ***B*)** Quantitative analysis of MBP mRNA expression in the hippocampus after lesioning. The time course of changes in mRNA expression after ECL was analyzed by in situ hybridization in the hippocampal neuropil. Data are expressed as the percentage of means of the optical density found in the adult nonlesioned controls. Results are given ± SD from 6 rats in each group (n = 12). Statistical significance is indicated by asterisks (*P<0.05; **P<0.01; ***P<0.001; Mann-Whitney U test).

Fig. 14

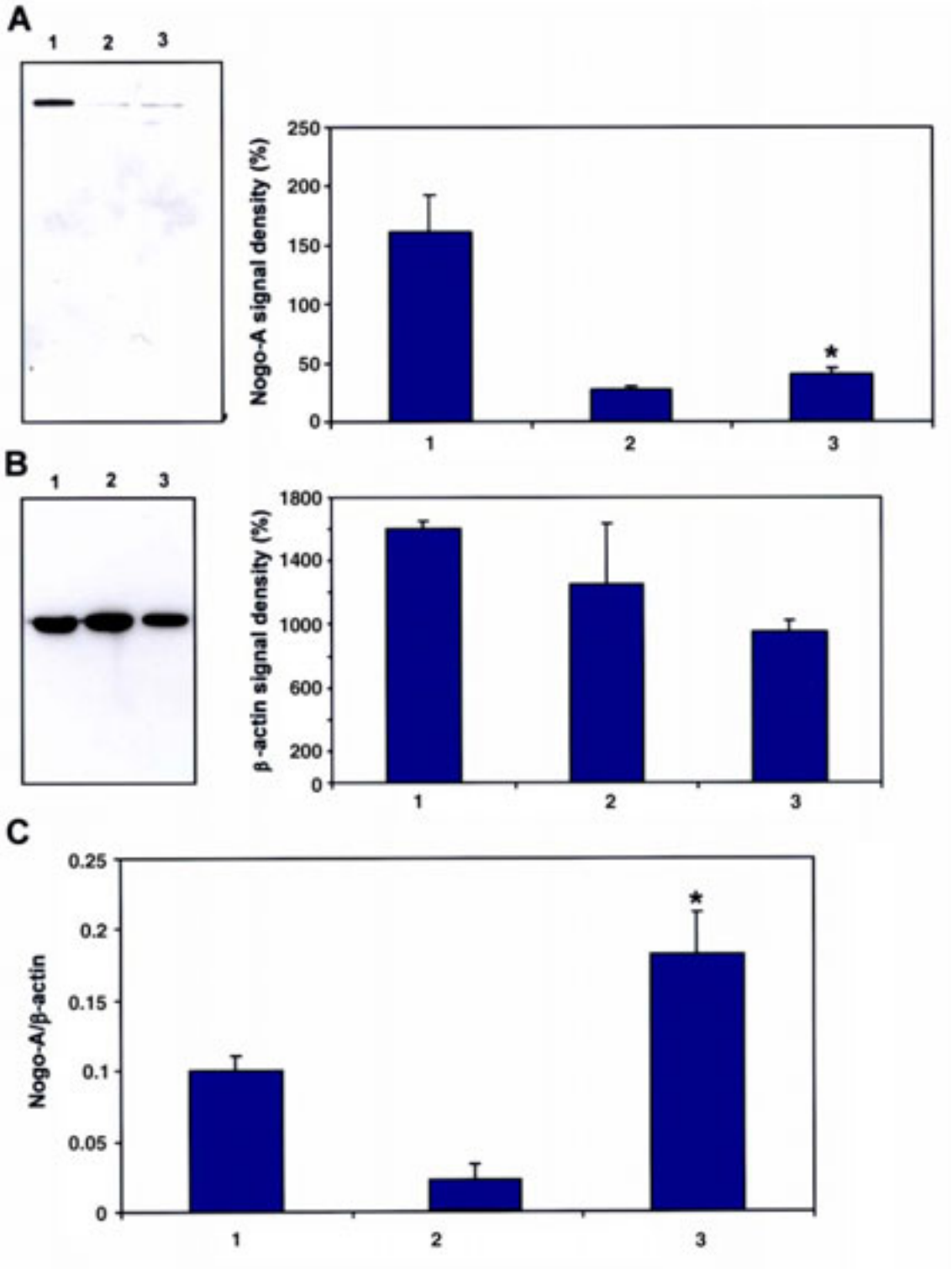

Figure 14. Nogo-A expression and quantitative analysis during development and after lesion. ***A*)** Nogo-A (205 kDa) protein levels and quantification in total protein extracts from postnatal hippocampus (1), adult hippocampus (2), and lesioned hippocampus 5 dal (3). ***B*)** β-Actin (42 kDa) expression levels and quantification shown for equal protein loading. ***C*)** Data from each experiment were quantified, and the ratio of Nogo-A to β-actin is given. Western blots were obtained on soluble total protein extracts by using the monoclonal antibody Nogo-A (α-C7) and β-actin. Data are expressed as the mean of three different experiments. Error bars represent ± SD. Statistical significance is indicated by asterisks (*P<0.05; **P<0.01; ***P<0.001; Mann-Whitney U test).

Fig. 15

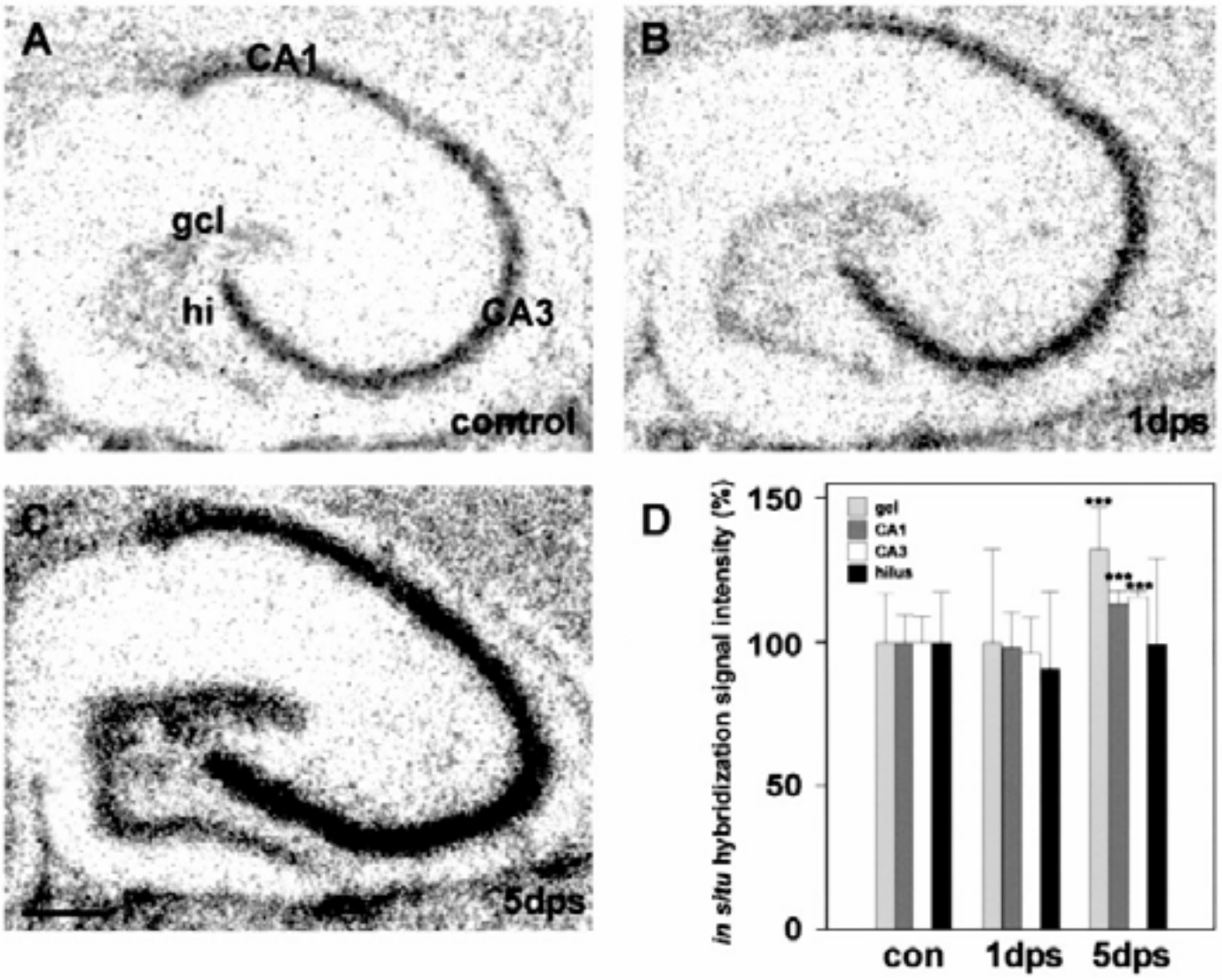

Figure 15. Nogo-A mRNA expression after kainate-induced seizures. ***A*)** Expression of Nogo-A transcripts in horizontal brain sections of adult nonlesioned controls (injected i.p. with saline), 1 dps (***B***), and 5 dps (***C***) as detected by in situ hybridization with the Nogo-A I oligonucleotide. Strong upregulation in CA1, CA3, and dentate gyrus was detectable at 5 dps. Scale bar = 400 µm. ***D*)** Quantitative analysis of Nogo-A mRNA expression in hippocampal cell layers. The time course of changes in mRNA expression after ECL was analyzed by in situ hybridization in the granule cell layer (gcl), CA1, CA3, and hilar region. Data are expressed as the percentage of means of the optical density found in the adult nonlesioned controls. Results are given ± SD from 5 rats in each group (n = 12). Statistical significance is indicated by asterisks (*P<0.05; **P<0.01; ***P<0.001; Mann-Whitney U test).

Fig. 16

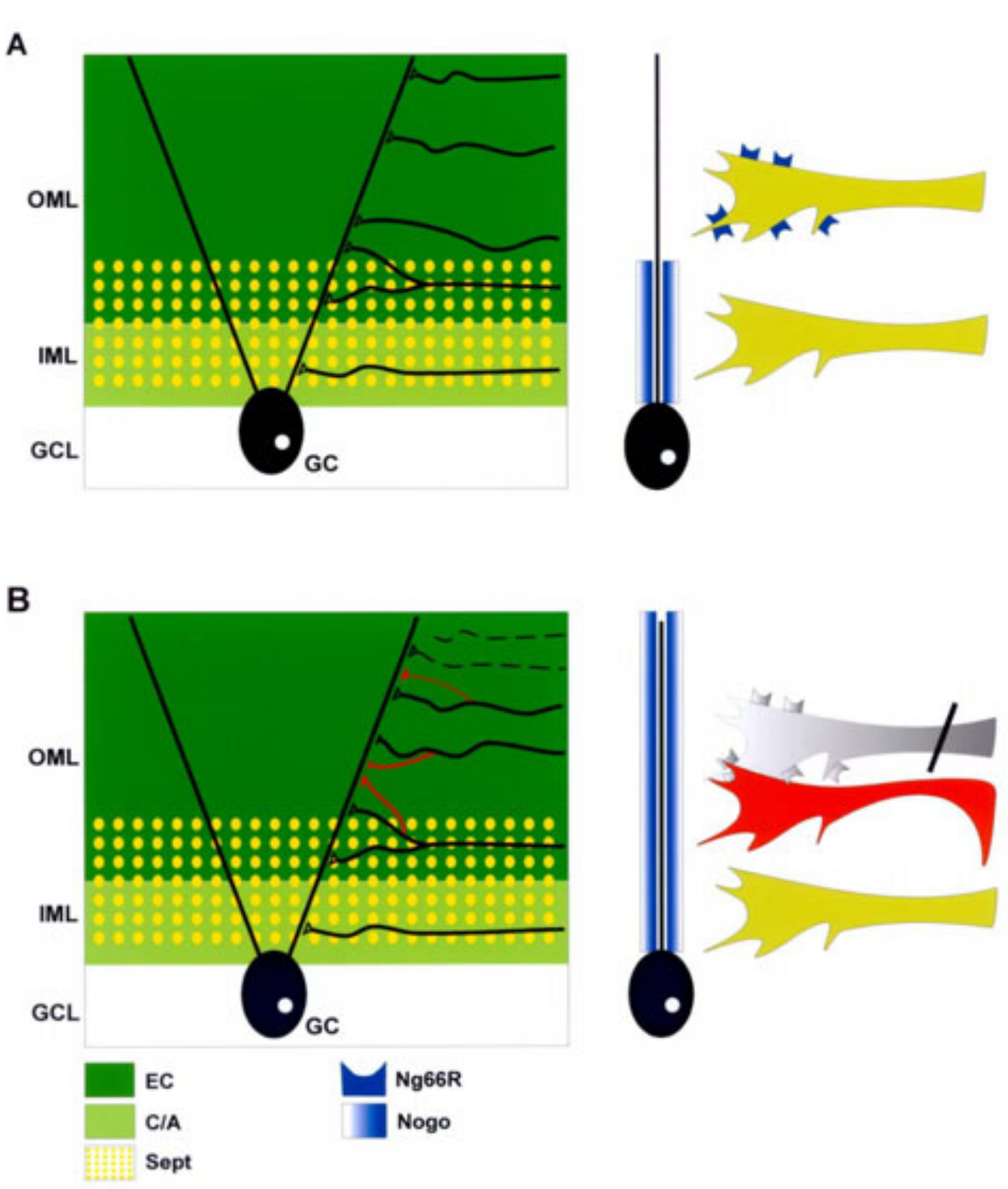

Figure 16. Summary of Nogo expression data in the hippocampus under control conditions (*A*) and after lesion (*B*). It is proposed that Nogo genes are expressed by granule cells (GC). Ng66R-expressing entorhinal axons are restricted to the outer molecular layer (OML) and do not enter the Nogo-rich inner molecular layer (IML). ***B*)** After lesioning, regrowing axons that do not bear the Ng66R can enter the Nogo-rich zone, which thereby leads to a replacement of lost entorhinal axons in the outer molecular layer. The decreased Ng66R expression correlates well with the time of axon growth into the lesioned hippocampus, if a transiently reduced axonal responsiveness to Nogo-A is assumed. The figure indicates the sources of the afferents coming from the EC, entorhinal projection; from the ipsilateral and contralateral hippocampus (C/A, commissural/associational fibers); Sept, septal projection; GCL, granule cell layer.